Getting just the supersymmetric standard model at intersecting branes on the $\mathbb{Z}_6$ orientifold

Gabriele Honecker[1,*] and Tassilo Ott[2,†]

[1]*Departamento de Física Teórica C-XI and Instituto de Física Teórica C-XVI, Universidad Autónoma de Madrid, Cantoblanco, 28049 Madrid, Spain*

[2]*Institute for Theoretical Physics, KULeuven, Celestijnenlaan 200 D, 3001 Leuven, Belgium*

(Received 23 April 2004; published 13 December 2004)

In this paper, globally $\mathcal{N} = 1$ supersymmetric configurations of intersecting D6-branes on the $\mathbb{Z}_6$ orientifold are discussed, involving also fractional branes. It turns out rather miraculously that one is led almost automatically to just *one* particular class of five stack models containing the standard model gauge group, which all have the same chiral spectrum. The further discussion shows that these models can be understood as exactly the supersymmetric standard model without any exotic chiral symmetric/antisymmetric matter. The superpartner of the Higgs finds a natural explanation and the hypercharge remains massless. However, the nonchiral spectrum within the model class is very different and does not in all cases allow for a $\mathcal{N} = 2$ low energy field theoretical understanding of the necessary breaking $U(1) \times U(1) \to U(1)$ along the Higgs branch, which is needed in order to get the standard Yukawa couplings. Also the left-right symmetric models belong to exactly *one* class of chiral spectra, where the two kinds of exotic chiral fields can have the interpretation of forming a composite Higgs. The aesthetical beauty of these models, involving only nonvanishing intersection numbers of an absolute value three, seems to be unescapable.

DOI: 10.1103/PhysRevD.70.126010 PACS numbers: 11.25.Mj, 12.60.Jv

I. INTRODUCTION

String Theory claims to be the correct unifying theory of gravity and elementary particle physics. As the latter, it should contain the standard model as a low energy limit, which is a chiral gauge theory. Since it was realized that chiral matter is possible in the context of intersecting D-branes [1], many different approaches have been taken, the most successful ones being constructions with intersecting D6-branes in type IIA orientifolds [2–13] (for recent reviews of the topic see [14–17]). The branes wrap special Lagrangian 3-cycles of the compact space in these models, which in general can be a simple toroidal, orbifolded or Calabi-Yau space, where the world sheet parity symmetry Ω together with a space-time symmetry $\mathcal{R}$ is modded out. In this picture, chiral fermions are localized at the intersections of the different stacks of D6-branes and consequently are 4-dimensional, whereas the gauge fields live on the whole world volume of the branes and by this are 7-dimensional. Finally, gravity is contained in the closed string sector of the theory and lives in the 10-dimensional bulk.

The massless chiral fermion spectrum can be determined in all three cases, as it only depends on the homology of the 3-cycles [18,19]. On the other hand, the nonchiral part of the spectrum depends on the closed string moduli and requires the world sheet conformal field theory computation of the one-loop amplitude that can be explicitly obtained only in the case of the torus or orbifolded torus. The 6-torus usually is assumed to be factorized in three 2-tori, i.e., $T^6 = T^2 \times T^2 \times T^2$. Every 3-cycle factorizes into three 1-cycles, one on every torus, and one obtains a nice geometrical picture.

In such an approach, a model containing only the standard model matter in the chiral sector has been obtained [20] (for similar subsequent models see [21,22]). But shortly afterwards, it was realized that this model is unstable due to the uncanceled $NS - NS$-tadpoles becoming manifest in the runaway behavior of the complex structure and dilaton moduli [23,24] (see also the remarks in [25]). The first instability can be cured by making the transition to a $\mathbb{Z}_3$-orientifold (where the exact realization of the standard model is different), but the dilaton instability cannot. Although this instability might be interesting from the perspective of cosmology and particularly inflation at first sight, it has been found, that only under very special and rather unsatisfactory requirements (for instance some moduli have to be fixed by an unknown mechanism), the remaining modulus could act as the inflaton [26] (for a different approach see, e.g., [27]). Beside that fact, inflation has to end and today only a very small cosmological constant is observed, which would require a very unnatural fine-tuning to comply with a natural time scale of for instance the dilaton instability.

Therefore, in the recent past another road has mainly been taken, namely, the attempt to construct instead a $\mathcal{N} = 1$ supersymmetric standard model (or supersymmetric SU(5) grand unified theory and Pati-Salam models, respectively). A first supersymmetric three-generation standardlike model has been constructed in [28,29]. Nevertheless, the goal so far has been achieved only with moderate success: either the constructions are plagued with a large amount of exotic chiral matter, as in

*Electronic address: gabriele@th.physik.uni-bonn.de
†Electronic address: tassilo.ott@fys.kuleuven.ac.be

the $\mathbb{Z}_2 \times \mathbb{Z}_2$ orientifold of [28–33], which might be cured by a confinement of the exotic chiral matter into composite fields coming from the strong infrared dynamics of the hidden sector [34,35]. In the other cases, brane recombinations of non-Abelian gauge groups are needed, as in the $\mathbb{Z}_4$ orientifold of [36] or the $\mathbb{Z}_4 \times \mathbb{Z}_2$ [37,38], giving rise to Pati-Salam models, and leading to nonflat and nonfactorizable branes which give up the complete predictability of the worldsheet conformal field theory approach. Another possibility are the constructions of [39,40], where only the sectors between certain branes are locally $\mathcal{N} = 1$-supersymmetric ("Q-SUSY" theories), but the setting as a whole is not, meaning that the $NS-NS$-tadpole is not canceled. For similar constructions see [41,42].

If a realistic globally $\mathcal{N} = 1$ supersymmetric standard model with the right chiral spectrum was found, many phenomenological properties could be discussed [43], such as for instance proton decay [44] or the running of the gauge couplings [34,45] and a possible gauge unification [46], the generation of masses [47–49], and the precise realization of the Higgs mechanism(s) [50] and Yukawa couplings [51–53], leading towards the goal of making contact with experimental reality [47]. It could even lead to an understanding of supersymmetry breaking [54,55].

Such a model can be compared to the minimal supersymmetric standard model (MSSM), which is claimed to be the best candidate for the search for supersymmetry at the LHC (for a good review see for instance [56]). This model has more predictive properties than a general supersymmetric standard model, it contains only a minimal Higgs sector of two SU(2) doublets and their superpartners whose hypercharge is exactly opposite, the declaration that all scalar masses are the same, all gaugino masses are the same, some statements about soft supersymmetry breaking (in the context of intersecting branes see [55]). In the past, the term MSSM often has been used very sloppily within string model building, basically meaning only the correct chiral spectrum. For a recent overview about the actual status of D6-brane constructions see [57,58].

A new possibility that has been explored is to get phenomenologically interesting models in a completely different corner of Calabi-Yau moduli space, namely, at the Gepner points [59–63]. Even chiral supersymmetric models with the standard model spectrum have been obtained already in this corner of moduli space [64] (for an introduction see [65]).

In this paper, the aim of getting a precise realization of a supersymmetric standard model will be continued furthermore on the compact space $T^6/\mathbb{Z}_6$, which again corresponds to a $\mathcal{N} = 2$ background of type II theory, following the classification of orbifolds in [66,67]. For this background (which geometrically can be defined in two different consistent ways on the 2-tori T_k^2), the $\mathbb{Z}_2$-twisted sector in both cases contributes a nonvanishing number $h_{2,1}$ to the number of complex structure deformations and so contains twisted 3-cycles, requiring the introduction of fractional branes [68,69], similar to the $\mathbb{Z}_4$-orientifold of [36].

The organization of the paper is as follows. The geometry of the orbifold is discussed in detail in Sec. II, including the definition of bulk and fractional cycles and an integral basis of homology, the orientifold plane and the resulting $R-R$-tadpole conditions for all possible choices of **A**- and **B**-tori.[1] Finally, the conditions for $\mathcal{N} = 1$ supersymmetry on the bulk and exceptional cycles are derived.

Section III discusses the calculation of the one-loop amplitudes and the transformation to the tree-channel, preparing the calculation of the chiral and nonchiral open string spectrum as well as clarifying the connection between the computation of cycles and string loop amplitudes.

Subsequently, there is a detailed discussion on anomalies and the generalized Green-Schwarz-mechanism in Sec. IV.

In Sec. V, we finally come to the systematic search of phenomenologically interesting models with a different number of stacks, leading to a detailed presentation of the explicit supersymmetric standard model which we have found in Sec. VI. There is also a short discussion on another possible left/right symmetric model in Sec. VII.

The conclusions and prospects are given in Sec. VIII.

Some technical details are collected in appendices A, B, C, and D.

II. GEOMETRY OF THE $T^6/\mathbb{Z}_6$ ORBIFOLD

In this section, the geometric setting of the six dimensional compact space including D6-branes, O6-planes, cancellation of $R-R$ tadpoles and supersymmetry are discussed.

If one assumes a factorization of the T^6 into three 2-tori, then the $T^6/\mathbb{Z}_6$ orbifold is generated by a rotation θ of the form

$$\theta: \qquad z^k \longrightarrow e^{2\pi i v_k} z^k \qquad \text{for } k = 1, 2, 3 \tag{1}$$

where the shift vector v is given by $v = (1/6, 1/6, -1/3)$, see for instance [66,67], and z^k is the complex coordinate on T_k^2.[2]

[1] They correspond to a vanishing or nonvanishing $NS-NS$ 2-form flux b in the T-dual F-flux picture of D9-branes.

[2] There exists a second, inequivalent possibility with $\mathbb{Z}_6$ symmetry, having the shift vector $v = (1/6, 1/3, -1/2)$, which is often denoted as $\mathbb{Z}_6'$. Both symmetric orbifolds in the IIA picture are T-dual to asymmetric orbifolds in the IIB background. Our models are therefore not T-dual to the symmetric $\mathbb{Z}_6$ orbifold of IIB in [70].

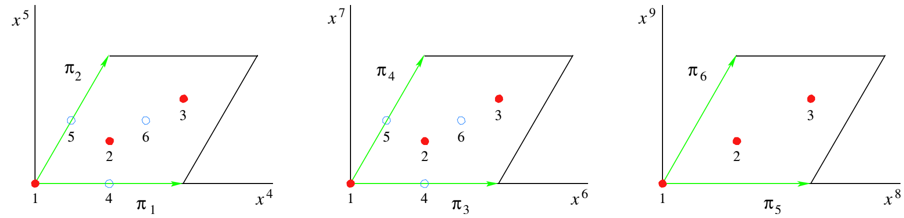

FIG. 1 (color online). Fixed points of the $T^6/\mathbb{Z}_6$ orbifold. Full circles denote θ^2 fixed points on $T_1^2 \times T_2^2$, empty circles additional θ^3 fixed points. On T_3^2, the points 1,2,3 are fixed under θ, the whole T_3^2 is fixed under θ^3. The coordinates are depicted for the **AAA** torus. The details of the choices of complex structures are given in Sec. II D and Appendix A.

Apart from the $\mathbb{Z}_6$ fixed points, additional points are fixed under the $\mathbb{Z}_3$ subsymmetry generated by θ^2. At all these fixed points, exceptional 2-cycles of zero volume[3] are stuck. Under the $\mathbb{Z}_2$ subsymmetry generated by θ^3, the whole third 2-torus T_3^2 is fixed, and exceptional 3-cycles which are products of 2-cycles stuck at the $\mathbb{Z}_2$ fixed points on $T_1^2 \times T_2^2$ times 1-cycles on the fix-torus T_3^2 appear. The geometry is depicted in Fig. 1, where a specific complex structure of the torus from six possibilities has been chosen. This is explained in more detail inII D appendix A.

The Hodge numbers of the $\mathbb{Z}_6$ orbifold are as follows (see e.g. [4] for the closed string spectrum, [72] for the number of untwisted and twisted moduli and [73] for the Hodge numbers explicitly),

$$\begin{aligned} h^U_{1,1} &= 5, \quad h^{\theta}_{1,1} = 3, \quad h^{\theta^2}_{1,1} = 15, \quad h^{\theta^3}_{1,1} = 6, \\ h^U_{2,1} &= 0, \quad h^{\theta}_{2,1} = 0, \quad h^{\theta^2}_{2,1} = 0, \quad h^{\theta^3}_{2,1} = 5. \end{aligned} \tag{2}$$

In the following, we will only consider the 3-cycles, but not the 2-cycles, since only intersections of D6-branes wrapping different 3-cycles in the compact dimensions give rise to chiral fermions. According to the value of the third Betti number, $b_3 = 2 + 2h_{2,1}$, two independent "bulk" 3-cycles are inherited from the six-torus and ten additional exceptional 3-cycles arise at the $\mathbb{Z}_2$ fix-points.

A. Bulk 3-cycles

Any basic factorizable 3-cycle on $\prod_{k=1}^3 T_k^2$ can be represented in terms of the basic 1-cycles of each 2-torus, π_{2k-1} and π_{2k}, as a direct product $\pi_{i,j,m} = \pi_i \otimes \pi_j \otimes \pi_m$. Out of the 2^3 different combinations, one can construct only two linearly independent bulk cycles which are invariant under the orbifold action. A convenient choice for them is given by

$$\begin{aligned} \rho_1 &= 2[(1 + \theta + \theta^2)\pi_{1,3,5}] \\ &= 2(\pi_{1,3,5} + \pi_{2,4,-6} + \pi_{2-1,4-3,6-5}) \\ &= 2(\pi_{1,4,5} + \pi_{1,3,6} + \pi_{2,3,5} - \pi_{1,4,6} - \pi_{2,4,5} - \pi_{2,3,6}), \\ \rho_2 &= 2[(1 + \theta + \theta^2)\pi_{2,3,5}] \\ &= 2(\pi_{2,3,5} + \pi_{2-1,4,-6} + \pi_{-1,4-3,6-5}) \\ &= 2(\pi_{1,4,5} + \pi_{1,3,6} + \pi_{2,3,5} - \pi_{1,3,5} - \pi_{2,4,6}). \end{aligned} \tag{3}$$

The factor of 2 in (3) arises due to the trivial action of θ^3 on any 3-cycle. Any orbifold invariant nonfactorizable 3-cycle can be written as a linear combination of these two bulk cycles.

The coefficients of the factorizable 3-cycles are determined by the wrapping numbers n_k and m_k along the basic 1-cycles π_{2k-1} and π_{2k} on the 2-torus T_k^2 and their orbifold images,

$$\begin{pmatrix} n_1 & m_1 \\ n_2 & m_2 \\ n_3 & m_3 \end{pmatrix} \xrightarrow{\theta} \begin{pmatrix} -m_1 & n_1 + m_1 \\ -m_2 & n_2 + m_2 \\ m_3 & -(n_3 + m_3) \end{pmatrix} \xrightarrow{\theta} \begin{pmatrix} -(n_1 + m_1) & n_1 \\ -(n_2 + m_2) & n_2 \\ -(n_3 + m_3) & n_3 \end{pmatrix}. \tag{4}$$

Starting with the 3-cycle $(n_1^a\pi_1 + m_1^a\pi_2) \otimes (n_2^a\pi_3 + m_2^a\pi_4) \otimes (n_3^a\pi_5 + m_3^a\pi_6)$ and adding its orbifold images, the invariant bulk 3-cycle is of the form

$$\Pi_a = Y_a\rho_1 + Z_a\rho_2, \tag{5}$$

where the coefficients Y_a and Z_a are given by linear combinations of products of the elementary wrapping numbers,

$$\begin{aligned} Y_a &\equiv n_1^a n_2^a n_3^a - \sum_{i\neq j\neq k\neq i} m_i^a m_j^a n_k^a - m_1^a m_2^a m_3^a, \\ Z_a &\equiv \sum_{i\neq j\neq k\neq i} m_i^a m_j^a n_k^a + \sum_{i\neq j\neq k\neq i} m_i^a n_j^a n_k^a. \end{aligned} \tag{6}$$

In computing the intersection numbers of the two independent bulk cycles which are invariant under a $\mathbb{Z}_N$ action, the orbifold projection has to be taken into account,

[3]The volume is not zero in the stringy sense, i.e., a nonvanishing string tension is generated by a discrete $NS - NS$ two-form background in the ten dimensional language. For more details see, e.g., the review article [71].

$$\Pi_a \circ \Pi_b = \frac{1}{N}\left(\sum_{i=0}^{N-1} \theta^i \pi_a\right) \circ \left(\sum_{j=0}^{N-1} \theta^j \pi_b\right). \qquad (7)$$

This leads to the intersection numbers of the two fundamental bulk cycles (3),

$$\rho_1 \circ \rho_2 = -2, \qquad \rho_1 \circ \rho_1 = \rho_2 \circ \rho_2 = 0, \qquad (8)$$

and for general bulk cycles $\Pi_a = Y_a \rho_1 + Z_a \rho_2$, we always obtain even intersection numbers,

$$I_{ab} \equiv \Pi_a \circ \Pi_b = 2(Z_a Y_b - Y_a Z_b). \qquad (9)$$

B. Exceptional 3-cycles

Exceptional 3-cycles in the orbifold limit only occur in the θ^3 sector. They consist of products of 2-cycles which are stuck at the $\mathbb{Z}_2$ fixed points and have zero volume in the orbifold limit on $T_1^2 \times T_2^2$ times a 1-cycle on T_3^2. The fixed point 1 in the origin of each 2-torus is already invariant under the orbifold generator θ. The other three $\mathbb{Z}_2$ fixed points are permuted by the $\mathbb{Z}_6$ symmetry in the following way,

$$\theta(4) = 5, \qquad \theta(5) = 6, \qquad \theta(6) = 4. \qquad (10)$$

Similarly, every 1-cycle on T_3^2 is invariant under θ^3, but the $\mathbb{Z}_6$ generator acts as follows,

$$\theta(\pi_5) = -\pi_6, \qquad \theta(\pi_6) = \pi_{5-6} = \pi_5 - \pi_6. \qquad (11)$$

Thus, the exceptional 3-cycles are given by orbifold invariant combinations of the products of 2- and 1-cycles,

$$\begin{aligned} &(1 + \theta + \theta^2)(e_{ij} \otimes \pi_k) \qquad \text{with} \\ &i, j = 1, 4, 5, 6; \quad k = 5, 6, \end{aligned} \qquad (12)$$

where the orbifold images are given by $\theta(e_{ij} \otimes \pi_k) = e_{\theta(i)\theta(j)} \otimes \theta(\pi_k)$. This ansatz leads to ten linearly independent exceptional cycles,

$$\begin{aligned}
\varepsilon_1 &= (e_{41} - e_{61}) \otimes \pi_5 + (e_{61} - e_{51}) \otimes \pi_6, & \tilde{\varepsilon}_1 &= (e_{51} - e_{61}) \otimes \pi_5 + (e_{41} - e_{51}) \otimes \pi_6, \\
\varepsilon_2 &= (e_{14} - e_{16}) \otimes \pi_5 + (e_{16} - e_{15}) \otimes \pi_6, & \tilde{\varepsilon}_2 &= (e_{15} - e_{16}) \otimes \pi_5 + (e_{14} - e_{15}) \otimes \pi_6, \\
\varepsilon_3 &= (e_{44} - e_{66}) \otimes \pi_5 + (e_{66} - e_{55}) \otimes \pi_6, & \tilde{\varepsilon}_3 &= (e_{55} - e_{66}) \otimes \pi_5 + (e_{44} - e_{55}) \otimes \pi_6, \\
\varepsilon_4 &= (e_{45} - e_{64}) \otimes \pi_5 + (e_{64} - e_{56}) \otimes \pi_6, & \tilde{\varepsilon}_4 &= (e_{56} - e_{64}) \otimes \pi_5 + (e_{45} - e_{56}) \otimes \pi_6, \\
\varepsilon_5 &= (e_{46} - e_{65}) \otimes \pi_5 + (e_{65} - e_{54}) \otimes \pi_6, & \tilde{\varepsilon}_5 &= (e_{54} - e_{65}) \otimes \pi_5 + (e_{46} - e_{54}) \otimes \pi_6.
\end{aligned} \qquad (13)$$

This construction resembles very much the one in [36]. The intersection numbers of exceptional cycles are computed from the self-intersection number -2 of any exceptional cycle e_{ij} stuck at a $\mathbb{Z}_2$ singularity and the intersection numbers of the 1-cycles on T_3^2, taking into account the factors from the orbifold projection similarly to Eq. (7). The result

$$\varepsilon_i \circ \tilde{\varepsilon}_j = -2\delta_{ij}, \qquad \varepsilon_i \circ \varepsilon_j = \tilde{\varepsilon}_i \circ \tilde{\varepsilon}_j = 0, \qquad (14)$$

leads to the intersection matrix for exceptional cycles

$$I_\varepsilon = \bigoplus_{j=1}^{5} \begin{pmatrix} 0 & -2 \\ 2 & 0 \end{pmatrix}. \qquad (15)$$

C. An integral basis

The intersection numbers of pure bulk cycles (8) and pure exceptional cycles (15) are always even. It is therefore possible to construct fractional cycles of the form $\frac{1}{2}\Pi^{\text{bulk}} + \frac{1}{2}\Pi^{\text{exceptional}}$ which form an unimodular lattice as required by Poincaré duality [74].

For example, a D6-brane with wrapping numbers $(n_1, m_1; n_2, m_2; n_3, m_3) = (1, 0; 1, 0; 1, 0)$ and its orbifold images wrap the bulk cycle ρ_1 and pass through the fixed points e_{kl} with $k, l \in \{1, 4\}$ as well as their orbifold images. The orbits of the three nontrivial fixed points e_{14}, e_{41}, e_{44} generate the exceptional cycles ε_1, ε_2, and ε_3 while the orbit of e_{11} vanishes. In this case, a valid fractional cycle is given by

$$\frac{1}{2}\rho_1 \pm \frac{1}{2}(\varepsilon_1 \pm \varepsilon_2 \pm \varepsilon_3) \qquad (16)$$

with arbitrary relative signs for the exceptional contributions.

This argument can be repeated for different wrapping numbers and 3-cycles which do not pass through e_{11} but instead are displaced by $\sum_{i=1}^{4} \sigma_i \pi_i$ (with $\sigma_i \in \{0, \frac{1}{2}\}$) from the origins of T_1^2 and T_2^2. All possible combinations of wrapping numbers of the bulk 3-cycles with fixed points are listed in Table XXIII. From this, we can obtain a basis for the unimodular lattice of 3-cycles

$$\alpha_1 = \frac{1}{2}\rho_1 + \frac{1}{2}(\varepsilon_1 + \varepsilon_2 + \varepsilon_3), \qquad \alpha_2 = \frac{1}{2}\rho_2 - \frac{1}{2}(\tilde{\varepsilon}_1 + \tilde{\varepsilon}_2 + \tilde{\varepsilon}_3), \qquad \alpha_3 = \frac{1}{2}\rho_1 + \frac{1}{2}(\varepsilon_1 - \varepsilon_2 + \varepsilon_3),$$
$$\alpha_4 = \frac{1}{2}\rho_2 - \frac{1}{2}(\tilde{\varepsilon}_1 - \tilde{\varepsilon}_2 + \tilde{\varepsilon}_3), \qquad \alpha_5 = \frac{1}{2}(\varepsilon_1 - \varepsilon_3 + \varepsilon_4 + \varepsilon_5), \qquad \alpha_6 = \frac{1}{2}(-\tilde{\varepsilon}_1 + \tilde{\varepsilon}_3 + \tilde{\varepsilon}_4 - \tilde{\varepsilon}_5),$$
$$\alpha_7 = \frac{1}{2}(\tilde{\varepsilon}_1 - \tilde{\varepsilon}_3 - \tilde{\varepsilon}_4 - \tilde{\varepsilon}_5), \qquad \alpha_8 = \frac{1}{2}(\varepsilon_1 - \varepsilon_3 + \varepsilon_4 - \varepsilon_5), \qquad \alpha_9 = -\frac{1}{2}\rho_1 + \frac{1}{2}(-\varepsilon_3 + \varepsilon_4 - \tilde{\varepsilon}_1 + \tilde{\varepsilon}_3 + 2\tilde{\varepsilon}_4),$$
$$\alpha_{10} = \frac{1}{2}\rho_2 + \frac{1}{2}(\varepsilon_1 - \varepsilon_3 + 2\varepsilon_4 - \tilde{\varepsilon}_1 + \tilde{\varepsilon}_4), \qquad \alpha_{11} = \frac{1}{2}(\rho_1 - \rho_2) + \frac{1}{2}(\varepsilon_1 + \varepsilon_4 + \tilde{\varepsilon}_3 + \tilde{\varepsilon}_4),$$
$$\alpha_{12} = \frac{1}{2}(-\rho_1 - 2\rho_2) + \frac{1}{2}(-\varepsilon_3 + \varepsilon_4 + \tilde{\varepsilon}_1 + \tilde{\varepsilon}_3), \tag{17}$$

with an intersection matrix

$$I_{\mathbb{Z}6} = \mathrm{diag}\left(\begin{pmatrix} 0 & 1 \\ -1 & 0 \end{pmatrix}, \cdots, \begin{pmatrix} 0 & 1 \\ -1 & 0 \end{pmatrix}\right). \tag{18}$$

The D6-branes of the IIA orientifold theory which we are going to consider can wrap fractional 3-cycles. The limitation on these cycles is determined by the O6-planes which will be discussed in the following section.

D. Orientifold projection

The aim of this work is to find stable and supersymmetric models. In order to cancel the $R-R$ charge of the D6-branes, orientifold 6-planes are required. Such O6-planes arise naturally, if the world sheet parity Ω is chosen to be accompanied by an antiholomorphic involution $\mathcal{R}$, which we can choose to be the complex conjugation

$$\mathcal{R}: \qquad z^k \to \bar{z}^k \qquad \text{for } k = 1, 2, 3, \tag{19}$$

where $z^k = x^{2+2k} + ix^{3+2k}$ are the complex coordinates on every 2-torus T^2_k.

1. Orientifold images of bulk cycles

In order to be consistent with the compactification, $\mathcal{R}$ has to be an automorphism of the $\mathbb{Z}_6$ invariant lattice. This leads to two possible orientations **A** and **B** of each 2-torus with a lattice basis and its dual which are given explicitly in appendix A. In terms of the notation of Fig. 1, the different orientations lead to the following projections of the fundamental 1-cycles under $\mathcal{R}$,

$$\mathbf{A}: \begin{cases} \pi_{2k-1} \xrightarrow{\mathcal{R}} \pi_{2k-1}, \\ \pi_{2k} \xrightarrow{\mathcal{R}} \pi_{2k-1} - \pi_{2k}, \end{cases} \qquad \mathbf{B}: \ \pi_{2k-1} \overset{\mathcal{R}}{\leftrightarrow} \pi_{2k}. \tag{20}$$

The geometry of the first two 2-tori is identical because the orbifold generator acts in the same way. Consequently, only six of the 2^3 naive choices are inequivalent while the choices **AB** and **BA** for $T^2_1 \times T^2_2$ lead to identical results. Evaluating the projection (20) on the right hand side of (3) leads to the orientifold images of bulk cycles displayed in Table I.

The bulk cycles which are invariant under $\mathcal{R}$ are easily read off from Table I. However, in order to determine the homology classes of the O6-planes and thereby the required sets of D6-branes, the factorizable 3-cycles have to be considered in more detail. The O6-planes can be decomposed into two orbits which are invariant under $\Omega\mathcal{R}\theta^{2k}$ and $\Omega\mathcal{R}\theta^{2k+1}$. The corresponding wrapping numbers, the coefficients Y and Z of the homological

TABLE I. $\mathcal{R}$ images of cycles inherited from the torus in the orbifold limit $T^6/(\mathbb{Z}_6 \times \Omega\mathcal{R})$.

	$\mathcal{R}$ images of bulk cycles	
Lattice	$\mathcal{R}$:ρ_1	$\mathcal{R}$:ρ_2
AAA	ρ_1	$\rho_1 - \rho_2$
AAB	ρ_2	ρ_1
ABA	ρ_2	ρ_1
ABB	$\rho_2 - \rho_1$	ρ_2
BBA	$\rho_2 - \rho_1$	ρ_2
BBB	$-\rho_1$	$\rho_2 - \rho_1$

TABLE II. O6-planes for $T^6/(\mathbb{Z}_6 \times \Omega\mathcal{R})$. In each case, the wrapping numbers of an arbitrary element of a $\mathbb{Z}_6$ orbit are listed. The coefficients Y, Z are computed from (6). The total homology class of the O6-planes is given by the sum over the two orbits for each lattice.

	O6-planes for $T^6/(\mathbb{Z}_6 \times \Omega\mathcal{R})$			
Lattice	$(n_1, m_1; n_2, m_2; n_3, m_3)$	Y	Z	Cycle
AAA	(1,0;1,0;1,0)	1	0	ρ_1
	(1,1;1,1;1,-1)	3	0	$3\rho_1$
AAB	(1,0;1,0;1,1)	1	1	$\rho_1 + \rho_2$
	(1,1;1,1;2,-1)	3	3	$3(\rho_1 + \rho_2)$
ABA	(1,0;1,1;1,0)	1	1	$\rho_1 + \rho_2$
	(1,1;0,1;1,-1)	1	1	$\rho_1 + \rho_2$
ABB	(1,0;1,1;1,1)	0	3	$3\rho_2$
	(1,1;0,1;2,-1)	0	3	$3\rho_2$
BBA	(1,1;1,1;1,0)	0	3	$3\rho_2$
	(0,1;0,1;1,-1)	0	1	ρ_2
BBB	(1,1;1,1;1,1)	-3	6	$3(-\rho_1 + 2\rho_2)$
	(0,1;0,1;2,-1)	-1	2	$-\rho_1 + 2\rho_2$

cycles [see Eq. (6)], and bulk cycles are listed in Table II. The overall cycle which is wrapped by the orientifold plane is given by the sum of the two orbits.

2. Orientifold images of exceptional cycles

In order to find the correct transformations of the fractional cycles and thereby the D6-branes under the orientifold projection, the transformations of the relevant fixed points on $T_1^2 \times T_2^2$ under $\mathcal{R}$ have to be taken into account,

$$\mathbf{A}: \begin{cases} 1 \xrightarrow{\mathcal{R}} 1, \\ 4 \xrightarrow{\mathcal{R}} 4, \\ 5 \overset{\mathcal{R}}{\leftrightarrow} 6, \end{cases} \qquad \mathbf{B}: \begin{cases} 1 \xrightarrow{\mathcal{R}} 1, \\ 4 \overset{\mathcal{R}}{\leftrightarrow} 5, \\ 6 \xrightarrow{\mathcal{R}} 6, \end{cases} \tag{21}$$

and the 1-cycle on T_3^2 transforms according to (20).

The images under the reflection $\mathcal{R}$ for all inequivalent lattices are displayed in Table III.

3. $R - R$-tadpole cancellation

The most important consistency requirement on the cohomology classes of the forms which live on the world volume of the D6-branes is that the charge of the $R - R$ 7-form which couples to the D6-branes and O6-planes vanishes. The Poincaré duals of these 7-forms are homology classes (see, e.g., [9]), implying that the $R - R$-tadpole cancellation conditions can be reformulated in terms of the bulk and exceptional 3-cycles discussed above.

The O6-planes only wrap bulk 3-cycles whereas D6-branes can wrap both exceptional and bulk 3-cycles. The general condition of an overall vanishing homology class is given by

$$\sum_a N_a(\Pi_a + \Pi_{a'}) - 4\Pi_{O6} = 0, \tag{22}$$

and can be evaluated in detail using Tables I and III where by $\Pi_{a'}$ we denote the $\mathcal{R}$ image of the 3-cycle Π_a. For the six inequivalent lattice orientations and only bulk branes we obtain

$$\begin{aligned}
\mathbf{AAA}&: \sum_a N_a(2Y_a + Z_a)\rho_1 = 2^4\rho_1,\\
\mathbf{AAB}&: \sum_a N_a(Y_a + Z_a)(\rho_1 + \rho_2) = 2^4(\rho_1 + \rho_2),\\
\mathbf{ABA}&: \sum_a N_a(Y_a + Z_a)(\rho_1 + \rho_2) = 2^3(\rho_1 + \rho_2),\\
\mathbf{ABB}&: \sum_a N_a(Y_a + 2Z_a)\rho_2 = 3\cdot 2^3\rho_2,\\
\mathbf{BBA}&: \sum_a N_a(Y_a + 2Z_a)\rho_2 = 2^4\rho_2,\\
\mathbf{BBB}&: \sum_a N_a Z_a(-\rho_1 + 2\rho_2) = 2^4(-\rho_1 + 2\rho_2).
\end{aligned} \tag{23}$$

Here, N_a is the number of D6-branes wrapping the cycle Π_a, the so-called stack size. These conditions are easily generalized for fractional D6-branes with a bulk part $\frac{1}{2} \times (Y_a\rho_1 + Z_a\rho_2)$ by inserting the corresponding factor $1/2$ on the left hand side of (23).

For exceptional cycles, the overall homology class has to cancel among all D6-branes and their $\mathcal{R}$-images by themselves, because the O6-plane does not contribute.

The same results can be obtained by computing the loop channel annulus, Möbius strip and Klein bottle amplitude and performing the modular transformation to the $R - R$-tree-channel. For more details on the open string amplitudes and massless spectrum see Sec. III.

E. Supersymmetry conditions

1. Supersymmetric bulk cycles

Factorizable 3-cycles preserve $\mathcal{N} = 1$ supersymmetry provided that the sum over the three angles with respect to the $\mathcal{R}$ invariant plane on all 2-tori vanishes. It is convenient to reformulate the supersymmetry condition in terms of the coefficients Y, Z [see Eq. (6)] as follows. If $\pi\varphi_a^k$ is the angle w.r.t. π_{2k-1} of the bulk cycle Π_a represented by the wrapping numbers (n_k^a, m_k^a), we have

$$\tan(\pi\varphi_a^k) = \sqrt{3}\frac{m_k^a}{2n_k^a + m_k^a}. \tag{24}$$

On an **A** lattice, $\pi\varphi_a^k$ is also the angle w.r.t. the $\mathcal{R}$ invariant axis, whereas on a **B** lattice it is given by $\pi\varphi_a^k - \frac{\pi}{6}$. We can combine both possibilities in the single equa-

TABLE III. $\mathcal{R}$ images of the exceptional cycles for $T^6/(\mathbb{Z}_6 \times \Omega\mathcal{R})$.

$\mathcal{R}$ images of exceptional cycles for $T^6/(\mathbb{Z}_6 \times \Omega\mathcal{R})$										
Lattice	$\mathcal{R}$:ε_1	$\mathcal{R}$:ε_2	$\mathcal{R}$:ε_3	$\mathcal{R}$:ε_4	$\mathcal{R}$:ε_5	$\mathcal{R}$:$\tilde\varepsilon_1$	$\mathcal{R}$:$\tilde\varepsilon_2$	$\mathcal{R}$:$\tilde\varepsilon_3$	$\mathcal{R}$:$\tilde\varepsilon_4$	$\mathcal{R}$:$\tilde\varepsilon_5$
AAA	ε_1	ε_2	ε_3	ε_5	ε_4	$\varepsilon_1 - \tilde\varepsilon_1$	$\varepsilon_2 - \tilde\varepsilon_2$	$\varepsilon_3 - \tilde\varepsilon_3$	$\varepsilon_5 - \tilde\varepsilon_5$	$\varepsilon_4 - \tilde\varepsilon_4$
AAB	$\tilde\varepsilon_1$	$\tilde\varepsilon_2$	$\tilde\varepsilon_3$	$\tilde\varepsilon_5$	$\tilde\varepsilon_4$	ε_1	ε_2	ε_3	ε_5	ε_4
ABA	ε_1	$\tilde\varepsilon_2 - \varepsilon_2$	ε_4	ε_3	ε_5	$\varepsilon_1 - \tilde\varepsilon_1$	$\tilde\varepsilon_2$	$\varepsilon_4 - \tilde\varepsilon_4$	$\varepsilon_3 - \tilde\varepsilon_3$	$\varepsilon_5 - \tilde\varepsilon_5$
ABB	$\tilde\varepsilon_1$	$-\varepsilon_2$	$\tilde\varepsilon_4$	$\tilde\varepsilon_3$	$\tilde\varepsilon_5$	ε_1	$\tilde\varepsilon_2 - \varepsilon_2$	ε_4	ε_3	ε_5
BBA	$\tilde\varepsilon_1 - \varepsilon_1$	$\tilde\varepsilon_2 - \varepsilon_2$	$\tilde\varepsilon_3 - \varepsilon_3$	$\tilde\varepsilon_5 - \varepsilon_5$	$\tilde\varepsilon_4 - \varepsilon_4$	$\tilde\varepsilon_1$	$\tilde\varepsilon_2$	$\tilde\varepsilon_3$	$\tilde\varepsilon_5$	$\tilde\varepsilon_4$
BBB	$-\varepsilon_1$	$-\varepsilon_2$	$-\varepsilon_3$	$-\varepsilon_5$	$-\varepsilon_4$	$\tilde\varepsilon_1 - \varepsilon_1$	$\tilde\varepsilon_2 - \varepsilon_2$	$\tilde\varepsilon_3 - \varepsilon_3$	$\tilde\varepsilon_5 - \varepsilon_5$	$\tilde\varepsilon_4 - \varepsilon_4$

tion $\pi\tilde{\varphi}_a^k = \pi(\varphi_a^k - \frac{b_k}{6})$, where $b_k = 0$ for an **A** and $b_k = 1$ for a **B** torus. The necessary condition for a supersymmetric factorizable bulk cycle is given in terms of the tangents by $\sum_{k=1}^3 \tan(\pi\tilde{\varphi}_a^k) = \prod_{k=1}^3 \tan(\pi\tilde{\varphi}_a^k)$. Evaluating this equation for the six inequivalent choices of lattice orientations and using (24), we obtain

$$\begin{aligned} &\mathbf{AAA}: Z_a = 0, && \mathbf{AAB}: Y_a - Z_a = 0, \\ &\mathbf{ABA}: Y_a - Z_a = 0, && \mathbf{ABB}: Y_a = 0, \\ &\mathbf{BBA}: Y_a = 0, && \mathbf{BBB}: 2Y_a + Z_a = 0. \end{aligned} \tag{25}$$

By the analysis of the angle criterion, we recover the result obtained by stating that the supersymmetric cycles are those special Lagrangian cycles which are calibrated w.r.t. the same holomorphic 3-form as the ones wrapped by the O6-planes. Stated differently, the vanishing coefficients in (25) are also those which are zero in Table II. Therefore, up to normalization the supersymmetric D6-branes wrap the same bulk 3-cycle as the O6-planes, and by this the intersection between the two always vanishes,

$$\Pi_a \circ \Pi_{O6} = 0. \tag{26}$$

There remains a little subtlety: since the tangent is periodic in π, the condition above does not distinguish between D6-branes and anti-D6-branes. However, a D6-brane gives a positive contribution to the untwisted $R - R$ charge on the left hand side of (23). The sufficient second condition for a supersymmetric bulk 3-cycle therefore reads

$$\begin{aligned} &\mathbf{AAA}, \mathbf{AAB}, \mathbf{ABA}: Y_a > 0, \\ &\mathbf{ABB}, \mathbf{BBA}, \mathbf{BBB}: Z_a > 0. \end{aligned} \tag{27}$$

2. Supersymmetry condition on exceptional cycles

Fractional branes preserve supersymmetry provided that their contribution from the exceptional cycles arises only from fixed points on the first two 2-tori which are traversed by the supersymmetric bulk part of the 2-cycle times a 1-cycle on T_3^2. All possible combinations of factorizable 2-cycles on $T_1^2 \times T_2^2$ and $\mathbb{Z}_2$ fixed points which they traverse are displayed in Table XXIII. The corresponding exceptional cycles can be read off from Table XXIV.

In all cases where the bulk part of the cycle passes through the origin of $T_1^2 \times T_2^2$, the signs of the contributions from the three nontrivial fixed points are arbitrary. However, if the bulk cycle does not pass through the origin, exceptional cycles arise from four nontrivial fixed points. In this case, three signs can be chosen independently while the fourth one is determined to be the product of the other three. This is due to the fact that relative Wilson lines $\frac{\tau_k}{2} \in \{0, 1/2\}$ between two branes are associated to the $\mathbb{Z}_2$ fixed points on T_k^2. Since in our convention, the fixed points are localized on $T_1^2 \times T_2^2$, discrete Wilson lines naturally occur on these two tori (compare also with [70]). We choose the convention such that for vanishing Wilson lines all fixed points contribute with the same sign. The relative signs between exceptional 2-cycles are then given as follows,

$$\begin{aligned} &\tau_0[e_{ik} + (-1)^{\tau_1} e_{jk} + (-1)^{\tau_2} e_{il} + (-1)^{\tau_1+\tau_2} e_{jl}] \\ &\quad = \tau_0 e_{ik} + \tau_1' e_{jk} + \tau_2' e_{il} + \tau_0 \tau_1' \tau_2' e_{jl}, \end{aligned} \tag{28}$$

where $\tau_0 = \pm 1$ is the global sign of contributions from exceptional cycles corresponding to the two possible $\mathbb{Z}_2$ eigenvalues and $\tau_k' = \tau_0(-1)^{\tau_k}$ for $k = 1, 2$. The allowed relative signs for combinations of exceptional 3-cycles associated to a specific bulk cycle are obtained by means of Table XXIV.

III. MASSLESS OPEN STRING SPECTRUM: TREE AND LOOP AMPLITUDES

The chiral spectrum and $R - R$-tadpole contributions can be computed from the 3-cycles the D6-branes wrap. However, to ensure that this method reproduces the string theory calculation it is crucial to understand the correspondence between the one-loop open string amplitudes which allow also for the computation of the nonchiral spectrum. The cycles are in direct correspondence to the boundary and cross-cap states of the tree-channel amplitudes, and the one-loop expressions are obtained via world sheet duality.

A stack of N_a identical fractional D6-branes in general supports the gauge group $U(N_a)$ and preserves $\mathcal{N} = 2$ supersymmetry by itself. This is in contrast to the compactifications on T^6 [5,6,20], $T^6/\mathbb{Z}_3$ [23], $T^6/(\mathbb{Z}_3 \times \mathbb{Z}_3)$, $T^6/(\mathbb{Z}_2 \times \mathbb{Z}_2)$ [28] and $T^6/(\mathbb{Z}_4 \times \mathbb{Z}_2)$ [37] which admit only pure bulk 3-cycles and hence preserve $\mathcal{N} = 4$ supersymmetry in the gauge sector. However, also on $T^6/\mathbb{Z}_6$, additional chiral multiplets in the adjoint representation arise at intersections of branes with their orbifold images as explained below.

The chiral part of the open string spectrum can be directly derived from the intersections of the 3-cycles in a given configuration as displayed in Table IV, whereas the knowledge of the nonchiral states such as Higgs particles in a standard model compactification or multiplets in the adjoint representation requires a detailed analysis of the string amplitudes or the computation of the Chan-Paton label for each massless open string state. Both techniques

TABLE IV. Generic chiral spectrum of intersecting D6-branes.

Multiplicity	Rep.
$\Pi_a \circ \Pi_b$	$(\mathbf{N}_a, \overline{\mathbf{N}}_b)$
$\Pi_a \circ \Pi_{b'}$	$(\mathbf{N}_a, \mathbf{N}_b)$
$\frac{1}{2}(\Pi_a \circ \Pi_{a'} - \Pi_a \circ \Pi_{O6})$	$\mathbf{Sym}_a$
$\frac{1}{2}(\Pi_a \circ \Pi_{a'} + \Pi_a \circ \Pi_{O6})$	$\mathbf{Anti}_a$

are briefly discussed in this section in order to show manifestly that our choice of Chan-Paton matrices and the sign of the orientifold projection on the exceptional cycles are appropriate. Furthermore, by using both techniques simultaneously, ambiguities in relative signs can be eliminated.

A. Boundary states for fractional intersecting branes

The untwisted and twisted boundary states are directly related to the bulk and exceptional cycles wrapped by fractional D6-branes. After applying a modular transformation on the scattering amplitudes between two D6-branes and between an O6-plane and a D6-brane, one obtains the two open string one-loop amplitudes, the annulus, and the Möbius strip. From these two, we can read off the complete massless spectrum.

The boundary state of an arbitrary fractional D6-brane consists of an untwisted part $|U_a\rangle$, corresponding to the wrapped bulk cycle $\Pi_a^{\rm bulk}$, and a twisted part $|T_a\rangle$, coming from the exceptional cycles $\Pi_a^{\rm ex}$ stuck at the traversed $\mathbb{Z}_2$ fixed points,

$$|B_a\rangle = |U_a\rangle + |T_a\rangle. \qquad (29)$$

For a pure bulk D6-brane, the complete boundary state is given by

$$|U_a\rangle = c_U\left(\prod_{k=1}^{3} L_k^a\right)\left[\sum_{l=0}^{2}|D6;\theta^l(n_i^a, m_i^a)\rangle\right], \qquad (30)$$

where in c_U all universal factors of the normalization have been absorbed.

$L_k^a = \sqrt{(n_k^a)^2 + n_k^a m_k^a + (m_k^a)^2}$ is the length of the 1-cycle wrapping T_k^2 measured in units of its radius R_k, and $\theta^l(n_i^a, m_i^a)$ labels a factorizable 3-cycle with wrapping numbers (n_i^a, m_i^a) $(i = 1, 2, 3)$ and its orbifold images.

A fractional brane wraps only $\frac{1}{2}\Pi_a^{\rm bulk}$. Accordingly, the normalization constant of the untwisted boundary state changes, $c_U \to c_U/2$, and the twisted parts of the boundary states are of the form

$$|T_a\rangle = c_T L_3^a \sum_{i,j}\alpha_{ij}\left[\sum_{l=0}^{2}|D6;\theta^l(n_3^a, m_3^a), \theta^l(e_{ij})\rangle\right] \qquad (31)$$

where all universal factors of the normalization have been absorbed in c_T. The relative factor c_T/c_U is fixed by world sheet duality. The twisted boundary states depend only on the wrapping numbers on T_3^2 and are stuck at those $\mathbb{Z}_2$ fixed points e_{ij} $(i, j = 1, 4, 5, 6)$ on $T_1^2 \times T_2^2$ which are traversed by the bulk cycle. The relative signs $\alpha_{ij} = \pm 1$ for different fixed points correspond to the $\mathbb{Z}_2$ eigenvalue and discrete Wilson lines displayed in Eq. (28).

The oscillator expansion of the boundary states and zero mode contributions in the annulus amplitude including discrete Wilson lines are stated in Appendix C.

The untwisted cross-cap states are constructed in a similar way to the boundary states. Since the total homology class of the O6-planes is composed of two independent orbits as shown in Table II, the cross-cap state contains two kinds of contributions,

$$|C\rangle = \mathcal{N}_{\rm even}\left(\sum_{k=0}^{2}|\Omega\mathcal{R}\theta^{2k}\rangle\right) + \mathcal{N}_{\rm odd}\left(\sum_{k=0}^{2}|\Omega\mathcal{R}\theta^{2k+1}\rangle\right), \qquad (32)$$

where the normalizations $\mathcal{N}_{\rm even}$, $\mathcal{N}_{\rm odd}$ depend on the choice of the lattice orientation and can be deduced from world sheet duality using the explicit calculation in [4]. In particular, for an **AB** lattice on $T_1^2 \times T_2^2$ they are identical.

From (30)–(32), the tree-channel annulus $\int_0^\infty \langle B_a|e^{-2\pi H_c l}|B_b\rangle$ and Möbius strip $\int_0^\infty \langle B_a|e^{-2\pi H_c l}|C\rangle + h.c.$ amplitudes can be computed and then transformed to the loop channel.

B. Loop channel amplitudes

The open string one-loop amplitudes are given by

$$\mathcal{A} + \mathcal{M} = c\int_0^\infty \frac{dt}{t^3}{\rm Tr}_{\rm open}[\mathbf{P}_{\rm orb}\mathbf{P}_{\rm GSO}\mathbf{P}_{\Omega\mathcal{R}}(-1)^{\mathbf{S}}e^{-2\pi t L_0}] \qquad (33)$$

with the projectors $\mathbf{P}_{\rm orb} = \frac{1}{6}\sum_{k=0}^{5}\theta^k$, $\mathbf{P}_{\rm GSO} = \frac{1}{2}\times[1 + (-1)^F]$, and $\mathbf{P}_{\Omega\mathcal{R}} = \frac{1}{2}(1 + \Omega\mathcal{R})$ and ${\rm Tr}_{\rm open}$ running over the NS and R sector weighted by $(-1)^{\mathbf{S}}$ where $\mathbf{S}$ is the space-time fermion number. The massless spectrum can be read off from (33) by a power series expansion.

In the following, we restrict to supersymmetric configurations and compute only the number of fermionic degrees of freedom.

1. Adjoint and bifundamental representations: Annulus

A general element of the orbifold group exchanges D6-branes with their images. Only a $\mathbb{Z}_2$ twist preserves the brane configuration, such that the only nonvanishing contributions to the annulus amplitude for bulk branes are given by

$$\mathcal{A} = \frac{c}{24}\int_0^\infty \frac{dt}{t^3}{\rm Tr}_{\rm open}\{(1 + \theta^3)[1 + (-1)^F] \times (-1)^{\mathbf{S}}e^{-2\pi t L_0}\}. \qquad (34)$$

The generic form of lattice contributions to the amplitudes per 2-torus is displayed in (C1) and the oscillator contributions are listed in (C5).

Since the R sector with $(-1)^F$ insertion always has a vanishing contribution to the loop channel amplitudes, the massless fermionic spectrum for bulk D6-branes at generic angles $\pi\varphi_k^{ab}$ is computed from

$$\mathcal{A}_R = \sum_{a,b} \frac{c}{24} \int_0^\infty \frac{dt}{t^3} [(2N_a)(2N_b) I_{ab} \mathcal{A}^{1/2,0}_{0,(\varphi_1^{ab},\varphi_2^{ab},\varphi_3^{ab})} + \mathrm{Tr}\gamma^a_{\theta^3} \mathrm{Tr}\gamma^{b,-1}_{\theta^3} I^{\theta^3}_{ab} \mathcal{A}^{1/2,0}_{v=1/2,(\varphi_1^{ab},\varphi_2^{ab},\varphi_3^{ab})}], \tag{35}$$

where $I_{ab} = \prod_{k=1}^3 (n_k^a m_k^b - n_k^b m_k^a)$ is the intersection number between the factorizable D6-branes a and b and $I^{\theta^3}_{ab}$ is the number of those intersections which are invariant under the θ^3 insertion, i.e., intersections localized at the $\mathbb{Z}_2$ fixed points e_{ij} on $T_1^2 \times T_2^2$ and with arbitrary position on T_3^2. One subtlety arises from the existence of the discrete Wilson lines: the $\mathbb{Z}_2$ invariant intersections are counted with relative signs which come from the Wilson lines. The matrices γ_{θ^3} are displayed below in Sec. III B 3, Eq. (39). For bulk branes, $\mathrm{Tr}\gamma^a_{\theta^3} = N_a - N_a = 0$, and $\mathbb{Z}_2$ insertions give vanishing contributions to the annulus amplitude. For fractional branes a, the coefficient of the contribution from the $\mathbb{1}$ insertion decreases by a factor of 2, i.e., replace $(2N_a) \to N_a$, in accordance with the expectation from the boundary state approach and $\mathrm{tr}\gamma^a_{\theta^3}$ is replaced by $\tau_0^a N_a$ where $\tau_0^a = \pm 1$ distinguishes the $\mathbb{Z}_2$ eigenvalues of the two fractional branes $\frac{1}{2}(\Pi_a^{\mathrm{bulk}} \pm \Pi_a^{\mathrm{ex}})$ forming a bulk brane.

For branes parallel on a 2-torus, in the above formula, the intersection number on the corresponding 2-torus is replaced by the appropriate lattice sum (C1) and the oscillator expression is modified as explained in Appendix C.3.

The annulus amplitude is sufficient to compute the massless spectrum of strings which are not invariant under the orientifold projection. This comprises the adjoint representations localized on a stack of identical branes or stuck at intersections of orbifold images as well as bifundamental representations at intersections of different branes a and b.

For N_a factional branes a which are not their own $\Omega\mathcal{R}$ image, the R sector annulus contributions containing adjoint representations are given by

$$\begin{aligned}
\mathcal{A}^R_{aa} &= \frac{c}{24} \int_0^\infty \frac{dt}{t^3} [N_a^2 \mathcal{L}_1^{\mathcal{A},a} \mathcal{L}_2^{\mathcal{A},a} \mathcal{L}_3^{\mathcal{A},a} \mathcal{A}^{1/2,0}_{0,(0,0,0)} + (\tau_0^a)^2 N_a^2 \mathcal{L}_3^{\mathcal{A},a} \mathcal{A}^{1/2,0}_{v=1/2,(0,0,0)}] \\
&= \frac{c}{24} \int_0^\infty \frac{dt}{t^3} [16 N_a^2 + \mathcal{O}(e^{-2\pi t})], \\
\mathcal{A}^R_{a(\Theta a)} &= \frac{c}{24} \int_0^\infty \frac{dt}{t^3} [N_a^2 I_{a(\Theta a)} \mathcal{A}^{1/2,0}_{0,(1/3,1/3,-2/3)} + (\tau_0^a)^2 N_a^2 I^{\theta^3}_{a(\Theta a)} \mathcal{A}^{1/2,0}_{v=1/2,(1/3,1/3,-2/3)}] \\
&= \frac{c}{24} \int_0^\infty \frac{dt}{t^3} [(2 I_{a(\Theta a)} + 2 I^{\theta^3}_{a(\Theta a)}) N_a^2 + \mathcal{O}(e^{-2\pi t/3})], \\
\mathcal{A}^R_{a(\Theta^2 a)} &= \frac{c}{24} \int_0^\infty \frac{dt}{t^3} [N_a^2 I_{a(\Theta^2 a)} \mathcal{A}^{1/2,0}_{0,(-1/3,-1/3,2/3)} + (\tau_0^a)^2 N_a^2 I^{\theta^3}_{a(\Theta^2 a)} \mathcal{A}^{1/2,0}_{v=1/2,(-1/3,-1/3,2/3)}] \\
&= \frac{c}{24} \int_0^\infty \frac{dt}{t^3} [(2 I_{a(\Theta^2 a)} + 2 I^{\theta^3}_{a(\Theta^2 a)}) N_a^2 + \mathcal{O}(e^{-2\pi t/3})].
\end{aligned} \tag{36}$$

It follows that the gauge group with support on N_a identical branes wrapping $\frac{1}{2}(\Pi_a^{\mathrm{bulk}} \pm \Pi_a^{\mathrm{ex}})$ is $U(N_a)$. The gauge sector preserves $\mathcal{N} = 2$ supersymmetry, i.e., one multiplet in the adjoint representation is living on the world volume of the stack of branes. This multiplet carries the degrees of freedom which correspond to a parallel displacement of the 1-cycle on the third torus. At each intersection of a with its orbifold images $(\theta^k a)$, one further chiral multiplet in the adjoint representation is stuck which is due to the fact that the orbifold images can recombine into a smooth cycle.

2. Symmetric and antisymmetric matter: Möbius strip

Arbitrary string configurations are not invariant under $\Omega\mathcal{R}$. However, some D6-branes can wrap the same 3-cycles as the O6-planes. In this case, the Möbius strip gives nonvanishing contributions to the gauge degrees of freedom and the resulting gauge group is special orthogonal.

Furthermore, strings can stretch between a brane a and an orbifold image in the orbit of the $\mathcal{R}$ image a'. These strings provide for further antisymmetric or symmetric representations of the unitary gauge factor with support on a.

The only nonvanishing R sector contributions to the Möbius strip are of the form

$$\mathcal{M}_R = \frac{c}{24} \int_0^\infty \frac{dt}{t^3} \{ \mathrm{Tr}^{R,aa'}_{\mathrm{open}} [\Omega\mathcal{R}(\mathbb{1} + \theta^3) e^{-2\pi t L_0}] + \mathrm{Tr}^{R,a(\theta a)'}_{\mathrm{open}} [\Omega\mathcal{R}(\theta + \theta^4) e^{-2\pi t L_0}] + \mathrm{Tr}^{R,a(\theta^2 a)'}_{\mathrm{open}} [\Omega\mathcal{R}(\theta^2 + \theta^5) e^{-2\pi t L_0}] \}. \tag{37}$$

They can be rewritten in terms of oscillator contributions and eigenvalues $\tau_k^a = \pm 1$ under $\Omega\mathcal{R}\theta^k$ as follows,

$$\mathcal{M}_R = \frac{c}{24}\int_0^\infty \frac{dt}{t^3}\sum_{k=0}^{2}\sum_{l=0,1}\tau^a_{k+3l}N_a I^{\mathcal{R}\theta^{k+3l}}_{a(\theta^k a)'} \times \mathcal{M}_{[\tilde{\varphi}_1+(k+3l)/6,\tilde{\varphi}_2+(k+3l)/6,\tilde{\varphi}_3-(k+3l)/3]} \quad (38)$$

where $\pi\tilde{\varphi}_k$ is the angle of brane a w.r.t. the $\mathcal{R}$ invariant axis as described in Sec. II E 1. $I^{\mathcal{R}\theta^{k+3l}}_{a(\theta^k a)'}$ counts the number of intersections between a and $(\theta^k a)'$ which are invariant under $\mathcal{R}\theta^{k+3l}$.

For example, let a and b be the fractional branes wrapping the bulk parts of the cycles on top of the O6-planes in the **AAB** model with wrapping numbers as displayed in Table II, i.e., $\Pi_a = \frac{1}{2}(\rho_1+\rho_2)+\frac{\tau_0^a}{2}\times(\varepsilon_1+\tilde{\varepsilon}_1+\varepsilon_2+\tilde{\varepsilon}_2+\varepsilon_3+\tilde{\varepsilon}_3)$ and $\Pi_b = \frac{3}{2}(\rho_1+\rho_2)-\frac{\tau_0^b}{2}(\varepsilon_1+\tilde{\varepsilon}_1+\varepsilon_2+\tilde{\varepsilon}_2+\varepsilon_3+\tilde{\varepsilon}_3)$ with $\tau_0^{a,b}=\pm 1$ being the two possible $\mathbb{Z}_2$ eigenvalues. The aa and bb strings support the gauge group $\mathrm{SO}(N_a)\times\mathrm{SO}(N_b)$ and one chiral multiplet in the antisymmetric representation, $\mathbf{Anti}_a+\mathbf{Anti}_b$. Furthermore, intersections of a with its orbifold images $(\theta^k a)$ $(k=1,2)$ provide for three multiplets in $\mathbf{Anti}_a$, and $b(\theta^k b)$ strings contribute 15 multiplets in $\mathbf{Anti}_b$. For $\tau_0^a=\tau_0^b$, ab and $a(\theta^2 b)$ strings carry three multiplets in $(\mathbf{N}_a,\mathbf{N}_b)$, and four multiplets in $(\mathbf{N}_a,\mathbf{N}_b)$ live on the $a(\theta b)$ strings. For $\tau_0^a=-\tau_0^b$, all sectors $a(\theta^k b)$ give vanishing contributions to the spectrum. Observe that this spectrum can be compared to the one arising from the branes c and e in Table XIV. In the latter case, the discrete relative Wilson on T_1^2 leads to a nonvanishing contribution to the spectrum although the $\mathbb{Z}_2$ eigenvalues differ.

3. Computation of the open spectrum from Chan-Paton labels

The open string spectrum at fractional D6-branes can be computed in a similar way as for bulk branes using the decomposition into irreducible representations of the orbifold group as follows.[4]

One choice of matrices consistent with the fact that the D6-branes a and b at the end of Sec. III B 2 carry orthogonal gauge factors and consequently $\Omega\mathcal{R}$ has to preserve the $\mathbb{Z}_2$ eigenvalues is given by

$$\gamma_{\theta^3} = \begin{pmatrix} \mathbb{1}_N & 0 \\ 0 & -\mathbb{1}_N \end{pmatrix}, \qquad \gamma_{\Omega\mathcal{R}} = \mathbb{1}_{2N}, \quad (39)$$

where N is the number of identical bulk branes. This choice confirms the global sign of the $\Omega\mathcal{R}$ projection on exceptional cycles in Table III, i.e., $\Omega\mathcal{R}$ acts merely as a permutation on exceptional 2-cycles but does not bring about any internal reflection of the blowups.

[4]See, e.g., [71] for a recent review on such decompositions in orbifold compactifications.

For an arbitrary kind of D6-branes wrapping a bulk 3-cycle which is not $\Omega\mathcal{R}\theta^k$ invariant, the resulting gauge group is $U(N)_1\times U(N)_2$. The two gauge factors belong to the two fractional branes whose superposition gives the bulk brane.

In particular, the aa strings decompose into $\mathbb{Z}_2$ even massless states $\psi^I_{-1/2}|0\rangle_{NS}$ for $I=\mu, 3, \overline{3}$ and their superpartners which provide for the vector multiplet carrying the gauge group and one chiral multiplet in the adjoint representation. For $I=1,\overline{1},2,\overline{2}$ the massless states are $\mathbb{Z}_2$ odd and correspond to strings stretching between the two fractional branes of opposite $\mathbb{Z}_2$ eigenvalues forming a bulk brane.

In the example at the end of Sec. III B 2, only one fractional cycle of each kind a and b occurs and therefore the $\mathbb{Z}_2$ odd states do not contribute to the massless spectrum on the brane. The representations of states localized at the intersections $a(\theta^k a)$ and $b(\theta^k b)$ with $k=1,2$ are computed from the fact that in this case the massless NS and R states are nondegenerate and $\mathbb{Z}_2$ invariant. The bulk parts of the cycles a and $(\theta^k a)$ intersect in three $\mathbb{Z}_2$ invariant points while b and $(\theta^k b)$ intersect in three $\mathbb{Z}_2$ invariant points and 24 points which form pairs under $\mathcal{R}$. Similarly, the ab and $a(\theta^2 b)$ massless states are nondegenerate and $\mathbb{Z}_2$ invariant while $a(\theta b)$ massless string states are twofold degenerate. By counting the respective intersections, the spectrum in Sec. III B 2 is recovered.

IV. ANOMALIES AND GREEN-SCHWARZ MECHANISM

As discussed in the previous section, the chiral spectrum and $R-R$-tadpole cancellation can be computed either via the 3-cycles or the string loop ampltidues, and the nonchiral spectrum by means of the latter method. The non-Abelian gauge factors remain unbroken in the low energy field theory, but the U(1) factors can have anomalies and acquire a mass via couplings to closed string $R-R$ fields. In this section, we discuss this generalized Green-Schwarz mechanism and show how to compute the surviving massless U(1) factors.

The closed string sector contains for all six different choices of lattice orientations the axion as untwisted $R-R$ scalar and five additional $R-R$ scalars from the θ^3 twisted sector. The number of vectors arising from the $R-R$ sectors depends on the lattice. The complete bosonic closed string spectrum is listed in Table V, the fermionic degrees of freedom follow from supersymmetry.

The axion and the five twisted $R-R$ scalars are those fields which participate in the generalized Green-Schwarz mechanism. Using the Tables I and III, the 3-cycles can be reexpressed in terms of $\mathcal{R}$ even and $\mathcal{R}$ odd linear combinations η_i and χ_j $(i,j=0,\ldots,5)$, respectively, with the property $\eta_i\circ\chi_j=-4\delta_{ij}$ and all other

TABLE V. Closed string spectrum on $T^6/(\mathbb{Z}_6 \times \Omega\mathcal{R})$: Counting of the bosonic degrees of freedom. The fermionic degrees of freedom follow from supersymmetry. 1 s. corresponds to a real scalar while 1 v. denotes a massless vector with its two helicities.

Closed string spectrum $T^6/(\mathbb{Z}_6 \times \Omega\mathcal{R})$												
Lattice	**AAA**		**AAB**		**ABA**		**ABB**		**BBA**		**BBB**	
Sector	$NS-NS$	$R-R$	$NS-NS$	$R-R$	$NS-NS$	$R-R$	$NS-NS$	$R-R$	$NS-NS$	$R-R$	$NS-NS$	$R-R$
Untwisted	$NS-NS$: Graviton + Dilaton + eight scalars; $R-R$: Axion + one vector											
$\theta+\theta^5$	4 s.	1 v.	6 s.	$\cdots$	4 s.	1 v.	6 s.	$\cdots$	4 s.	1 v.	6 s.	$\cdots$
$\theta^2+\theta^4$	20 s.	5 v.	30 s.	$\cdots$	18 s.	6 v.	24 s.	3 v.	20 s.	5 v.	30 s.	$\cdots$
θ^3	$NS-NS$: 15 scalars; $R-R$: five scalars + one vector											

intersections being trivial. The detailed form of these linear combinations depends on the choice of the lattice as listed in Tables VI and VII.

A general 3-cycle and its $\mathcal{R}$ image can be rewritten in terms of the $\mathcal{R}$ even and odd cycles as follows,

$$\Pi_a = \sum_{i=0}^{5}(r_a^i\eta_i + s_a^i\chi_i), \qquad \Pi_{a'} = \sum_{i=0}^{5}(r_a^i\eta_i - s_a^i\chi_i), \tag{40}$$

with r_a^i, s_a^i multiples of one quarter. The $R-R$-tadpole cancellation condition (22) can be rephrased in terms of these coefficients as

$$\sum_b 2N_b\vec{r}_b = 4\vec{r}_{O6} \tag{41}$$

with $\vec{r}_{O6} = (r_{O6}^0, 0, 0, 0, 0, 0)^T$ and r_{O6}^0 as read off from Table II. Using the fact that the intersection number of two arbitrary 3-cycles is given by $\Pi_a \circ \Pi_b = 2(-\vec{r}_a\cdot\vec{s}_b + \vec{s}_a\cdot\vec{r}_b)$, and multiplying (41) by $2\vec{s}_a$ leads to

$$\begin{aligned} 0 &= 4N_a\vec{s}_a\cdot\vec{r}_a - 8\vec{s}_a\cdot\vec{r}_{O6} + 4\sum_{b\neq a}N_b\vec{s}_a\cdot\vec{r}_b \\ &= N_a\Pi_a\circ\Pi_{a'} - 4\Pi_a\circ\Pi_{O6} + \sum_{b\neq a}N_b(\Pi_a\circ\Pi_b \\ &\quad +\Pi_a\circ\Pi_{b'}). \end{aligned} \tag{42}$$

As in the toroidal orientifold models with intersecting D6-branes [20], Eq. (42) shows manifestly that the $R-R$-tadpole cancellation conditions imply the disappearance of all cubic gauge anomalies of the generic spectrum listed in Table IV and impose analogous conditions for matter charged under SU(2) and U(1) factors.

The mixed gauge anomalies are of the form

$$\begin{aligned} \mathcal{A}_{\mathrm{U}(1)_a-\mathrm{SU}(N_b)^2} = 4\vec{s}_a\cdot\Bigg[\vec{r}_bN_a + \delta_{ab}\bigg(\sum_c N_c\vec{r}_c \\ - 2\vec{r}_{O6}\bigg)\Bigg]C_2(N_b). \end{aligned} \tag{43}$$

The inner bracket in (43) vanishes upon $R-R$-tadpole cancellation. The remaining part which is also present for $a\neq b$ is compensated by the generalized Green-Schwarz couplings as follows. Six linearly independent $\Omega\mathcal{R}$ even $R-R$ scalars and their dual two-forms can be defined as the pull back of the ten dimensional Ω even 3-form and the Ω odd 5-form over the $\mathcal{R}$ even and $\mathcal{R}$ odd 3-cycles, respectively,

$$\tilde{\phi}_i = (4\pi^2\alpha')^{-3/2}\int_{\eta_i} C_3, \qquad \tilde{B}_2^i = (4\pi^2\alpha')^{-3/2}\int_{\chi_i} C_5. \tag{44}$$

The axion of Table V corresponds to $\tilde{\phi}_0$ while the remaining scalars $\tilde{\phi}_1, \ldots, \tilde{\phi}_5$ represent the five $R-R$ scalars from the θ^3 twisted sector.

The four dimensional effective couplings to the gauge fields are determined by the coefficients of the 3-cycles in (40),

TABLE VI. $\mathcal{R}$ even cycles for $T^6/(\mathbb{Z}_6\times\Omega\mathcal{R})$.

	$\mathcal{R}$ even cycles for $T^6/\mathbb{Z}_6$					
Lattice	η_0	η_1	η_2	η_3	η_4	η_5
AAA	ρ_1	ε_1	ε_2	ε_3	$\varepsilon_4+\varepsilon_5$	$-\tilde{\varepsilon}_4-\varepsilon_5+\tilde{\varepsilon}_5$
AAB	$\rho_1+\rho_2$	$\varepsilon_1+\tilde{\varepsilon}_1$	$\varepsilon_2+\tilde{\varepsilon}_2$	$\varepsilon_3+\tilde{\varepsilon}_3$	$-\tilde{\varepsilon}_4-\varepsilon_5$	$-\varepsilon_4-\tilde{\varepsilon}_5$
ABA	$\rho_1+\rho_2$	ε_1	$-\tilde{\varepsilon}_2$	ε_5	$\varepsilon_3+\varepsilon_4$	$-\tilde{\varepsilon}_3-\varepsilon_4+\tilde{\varepsilon}_4$
ABB	ρ_2	$\varepsilon_1+\tilde{\varepsilon}_1$	$\varepsilon_2-2\tilde{\varepsilon}_2$	$\varepsilon_5+\tilde{\varepsilon}_5$	$-\tilde{\varepsilon}_3-\varepsilon_4$	$-\varepsilon_3-\tilde{\varepsilon}_4$
BBA	ρ_2	$-\tilde{\varepsilon}_1$	$-\tilde{\varepsilon}_2$	$-\tilde{\varepsilon}_3$	$\varepsilon_4-\varepsilon_5+\tilde{\varepsilon}_5$	$-\tilde{\varepsilon}_4-\tilde{\varepsilon}_5$
BBB	$-\rho_1+2\rho_2$	$\varepsilon_1-2\tilde{\varepsilon}_1$	$\varepsilon_2-2\tilde{\varepsilon}_2$	$\varepsilon_3-2\tilde{\varepsilon}_3$	$\varepsilon_4-\varepsilon_5$	$-\tilde{\varepsilon}_4+\varepsilon_5-\tilde{\varepsilon}_5$

TABLE VII. $\mathcal{R}$ odd cycles for $T^6/(\mathbb{Z}_6 \times \Omega\mathcal{R})$.

Lattice	$\mathcal{R}$ odd cycles for $T^6/\mathbb{Z}_6$					
	χ_0	χ_1	χ_2	χ_3	χ_4	χ_5
AAA	$-\rho_1 + 2\rho_2$	$-\varepsilon_1 + 2\tilde{\varepsilon}_1$	$-\varepsilon_2 + 2\tilde{\varepsilon}_2$	$-\varepsilon_3 + 2\tilde{\varepsilon}_3$	$\tilde{\varepsilon}_4 - \varepsilon_5 + \tilde{\varepsilon}_5$	$\varepsilon_4 - \varepsilon_5$
AAB	$-\rho_1 + \rho_2$	$-\varepsilon_1 + \tilde{\varepsilon}_1$	$-\varepsilon_2 + \tilde{\varepsilon}_2$	$-\varepsilon_3 + \tilde{\varepsilon}_3$	$\varepsilon_4 - \tilde{\varepsilon}_5$	$-\tilde{\varepsilon}_4 + \varepsilon_5$
ABA	$-\rho_1 + \rho_2$	$-\varepsilon_1 + 2\tilde{\varepsilon}_1$	$2\varepsilon_2 - \tilde{\varepsilon}_2$	$-\varepsilon_5 + 2\tilde{\varepsilon}_5$	$\tilde{\varepsilon}_3 - \varepsilon_4 + \tilde{\varepsilon}_4$	$\varepsilon_3 - \varepsilon_4$
ABB	$-2\rho_1 + \rho_2$	$-\varepsilon_1 + \tilde{\varepsilon}_1$	ε_2	$-\varepsilon_5 + \tilde{\varepsilon}_5$	$\varepsilon_3 - \tilde{\varepsilon}_4$	$-\tilde{\varepsilon}_3 + \varepsilon_4$
BBA	$-2\rho_1 + \rho_2$	$2\varepsilon_1 - \tilde{\varepsilon}_1$	$2\varepsilon_2 - \tilde{\varepsilon}_2$	$2\varepsilon_3 - \tilde{\varepsilon}_3$	$\tilde{\varepsilon}_4 - \tilde{\varepsilon}_5$	$\varepsilon_4 - \tilde{\varepsilon}_4 + \varepsilon_5$
BBB	$-\rho_1$	ε_1	ε_2	ε_3	$-\varepsilon_4 + \tilde{\varepsilon}_4 - \tilde{\varepsilon}_5$	$\varepsilon_4 + \varepsilon_5$

$$\sum_{i=0}^{5} 2r_b^i \int_{M_4} \tilde{\phi}_i \mathrm{tr} F_b \wedge F_b, \qquad N_a \sum_{i=0}^{5} 2s_a^i \int_{M_4} \tilde{B}_i \wedge \mathrm{tr} F_a, \tag{45}$$

the factor of 2 stemming from the couplings to branes a as well as their images a'. The couplings in (45) obviously match those in (43) and thus provide for the cancellation of mixed gauge anomalies.

In order for a U(1) factor $Q = \sum_a x_a Q_a$ to remain massless, the couplings to all two-forms have to vanish, i.e., the coefficients x_a have to fulfill

$$\sum_a x_a N_a \vec{s}_a = 0. \tag{46}$$

In a generic model, at most six Abelian gauge factors can acquire a mass. However, in a supersymmetric setup all couplings to $\tilde{B}_0$ vanish and only up to five Abelian factors can become massive.

The nonanomalous U(1)s can also be calculated directly from the homological cycles by determining the kernel of the matrix [14,15]

$$M_{aI} = N_a(v_a^I - v_a^{I\prime}), \tag{47}$$

where v_a^I and $v_a^{I\prime}$ are just the 12 coefficients of the homological basis and the $\Omega\mathcal{R}$-mirror, respectively; a runs overall stacks of branes.

V. SUPERSYMMETRIC MODELS

After having specified the $R-R$-tadpole and supersymmetry conditions, it is now possible to search for concrete configurations of fractional D6-branes fulfilling these conditions.

In this section, we explore systematically what kind of gauge groups and chiral spectra can be obtained. To do so, we will proceed in the usual way for a certain number r of stacks, each consisting of N_r branes. Our main aim is to find a phenomenologically appealing supersymmetric three generation model, ideally without any exotic chiral matter as compared to the standard model.

The guiding model for our considerations will be the nonsupersymmetric standard model on the toroidal orientifold of [20] which might also allow for a supersymmetric extension. It has the two main features that first, it only contains exactly the standard model matter as chiral matter (plus right-handed neutrinos) and second, only in bifundamental representations of the gauge groups. This model is realized on four stacks plus possibly hidden branes (which do not intersect with the standard model branes). The second different possibility to realize the standard model from [23] does not have a supersymmetric extension on the $\mathbb{Z}_6$-orientifold for the following reason: in this model, the right-handed u, c, and t quarks have been realized in the antisymmetric representation of the U(3) brane and it was not allowed to have any symmetric representations of this gauge factor. In the present case, the intersection of any brane cycle Π_a with the orientifold plane Π_{O6} has to vanish for a supersymmetric model, i.e., $\Pi_a \circ \Pi_{O6} = 0$. But according to Table IV, this just means that the number of symmetric and antisymmetric representations on a certain brane are always the same.

In the past, the model building approaches often have been rather nonsystematic, a fact that we will try to avoid here. To do so, a computer program has been set up in order to first calculate the configurations in terms of wrapping numbers n and m which fulfill the untwisted $R-R$-tadpole conditions and the supersymmetry conditions at the same time, where we have to keep in mind that only the untwisted $R-R$-tadpole conditions get a contribution from the orientifold planes.

Having specified all such configurations in a certain range of wrapping numbers, all possible fractional cycles are constructed after a reduction to one representant of the orbit. This of course has to be done according to the specific fixed points that the particular fractional brane passes through. The possible cycles can be determined from Table XXIII, where we have allowed a displacement of the branes from the origin by

$$\sum_{i=1}^{4} \sigma_i \pi_i \quad \text{with} \quad \sigma_i \in \left\{0, \frac{1}{2}\right\} \tag{48}$$

on the first two T^2, according to the discussion in the preceding sections. For every given configuration of

TABLE VIII. All possible intersection numbers $(I_{ab}, I_{ab'})$ between two stacks of branes a and b for intersections with only bifundamental representations of the gauge group.

$(I_{ab}, I_{ab'})$										
(0, 0)	$(\pm 1, \pm 1)$	$(\pm 2, \pm 2)$	$(\pm 3, \pm 3)$	$(\pm 5, \pm 5)$	$(0, \pm 1)$	$(\pm 1, 0)$	$(0, \pm 3)$	$(\pm 3, 0)$	$(\pm 1, \pm 3)$	$(\pm 3, \pm 1)$

wrapping numbers fulfilling the $R-R$-tadpole conditions in the untwisted part, this procedure allows for a number of $16 \cdot 2^3 = 128$ different cycles according to Eq. (28) and Table XXIII for every stack. This enhances the model building possibilities by a factor of 128^r (where r again is the number of stacks) as compared to the case of constructions without fractional cycles (like in the $\mathbb{Z}_3$ orientifold of [23]). The reader should be reminded that the fulfillment of the untwisted $R-R$-tadpole equation actually does not depend on the specific choices of wrapping numbers n and m for every stack of branes, but only on the corresponding coefficients of the two homological cycles Y_a and Z_a which are defined in Eq. (6). In contrast, the construction of twisted cycles does depend on the numbers n and m, but actually only on the oddness and evenness of the wrapping numbers on the first two tori. These two facts allow for a more effective and evolved computer algorithm to handle the amount of computation.

To get started, we will look for all generally possible two stack configurations (which for now shall be denoted a and b). We will not require to fulfill the $R-R$-tadpole equation at this point, therefore we do not have to specify the size N_r for any of these two stacks. In this way we get the most general intersection numbers which—most optimistically—are possible in any $\mathbb{Z}_6$ orientifold construction (with more than one stack). These intersection numbers make up a finite set, if we insist on constructions without anti-D-branes, simply because every D-brane gives a positive contribution which never should be larger than the absolute value of the contribution from the orientifold plane. This gives an upper bound on Y_a and Z_a if one assumes the smallest possible stack size of $N_a = 1$. The computation shows that the possibilities completely agree on all possible tori. They are listed in Table VIII for the case that the intersections of the two branes with themselves and their orientifold mirror brane are vanishing, i.e., $I_{aa} = I_{aa'} = I_{bb} = I_{bb'} = 0$.[5] This means that we require that there are no symmetric and antisymmetric representations in the corresponding open string sectors. Another computation shows that exactly the same intersections are still possible if we additionally insist on $\mathcal{N} = 1$ supersymmetry on both stacks.

We can already see from Table VIII, that an identical construction of the standard model spectrum to the one in [20] also will not be possible: one cannot get a pair of intersection numbers between two stacks of the form $(I_{ab}, I_{ab'}) = (1, 2)$. In the model in [20], this possibility was necessary in order to realize the three generations of left-handed quarks as two SU(2) doublets and one anti-doublet. In this way, no additional (w.r.t. the standard model) SU(2) lepton doublets were required in order to cancel the U(2) anomaly in the effective 4-dimensional gauge sector.

This problem seems to persist in the construction on the $\mathbb{Z}_6$ orientifold, but later we will see how it actually can be overcome and that we can even profit from this fact. At this point, it just shall be mentioned that this might only be a problem in a construction with four observable intersecting (plus hidden) stacks.

Before coming to the most interesting five stack configurations, we will shortly mention some results on 2, 3, and 4 stack configurations and how they automatically point towards a five stack model.

A. 2, 3, and 4 stack configurations

Even with two stacks of various stack sizes, already nontrivial models which fulfill the $R-R$-tadpole cancellation conditions and carry matter in bifundamental representations can be obtained. But in all such models on all six different tori, the stack size of both stacks has to agree. Besides, there also exists matter in the symmetric and antisymmetric representation of at least one gauge factor and furthermore, only even intersection numbers are possible. This means that the number of bifundamental representations is always even, too. A typical example for $N_a = N_b = 3$ on the **AAA**-torus is given in Table IX.

These limitations can be explained by the simple fact that the twisted homological cycles plus their $\mathcal{R}$-mirrors have to be exactly opposite to each other for the two stacks. Therefore, one cannot obtain any 3-generation model like the SU(5)-grand unified theory model in [23] and one has to allow for at least three stacks for a phenomenologically appealing model.

There is a simple possibility how to sort out right from the start which stack sizes are able to give valid models and which are not. Indeed, only the first two components of the $R-R$-tadpole Eq. (22) which do not depend on the construction of fractional cycles, are already enough to rule out most of the possibilities, because if there are no solutions for a given stack size, the fractional cycles cannot change this. On the other hand, if there are solutions of the untwisted $R-R$-tadpole components, it is not ensured that the twisted $R-R$-tadpole components also admit solutions.

[5] In fact, the intersection number of any brane with itself vanishes automatically in four dimensions.

TABLE IX. The wrapping numbers and homology cycles of the D6-branes in a 2-stack model containing chiral matter.

Stack	(n_I, m_I)	Homology cycle	Chiral spectrum
U(3)	$(-3, 1; -3, 2; -1, 1)$	$\Pi_1 = \frac{1}{2}(7\rho_2 - \varepsilon_1 - \varepsilon_3 + 2\tilde{\varepsilon}_1 + \tilde{\varepsilon}_3 + \tilde{\varepsilon}_5)$	$2 \times (\bar{\mathbf{3}}, \mathbf{3})$
		$\Pi_1' = \frac{1}{2}(7\rho_2 + 2\varepsilon_1 + \varepsilon_4 + \varepsilon_5 - \tilde{\varepsilon}_1 - \tilde{\varepsilon}_4)$	$1 \times (\mathbf{3}_A, 1), 1 \times (\mathbf{6}_S, 1)$
			$1 \times (1, \bar{\mathbf{3}}_A), 1 \times (1, \bar{\mathbf{6}}_S)$
U(3)	$(0, -1; 0, 1; -1, 1)$	$\Pi_2 = \frac{1}{2}(\rho_2 - 2\varepsilon_1 - \varepsilon_4 - \varepsilon_5 + \tilde{\varepsilon}_1 + \tilde{\varepsilon}_4)$	
		$\Pi_2' = \frac{1}{2}(\rho_2 + \varepsilon_1 + \varepsilon_3 - 2\tilde{\varepsilon}_1 - \tilde{\varepsilon}_3 - \tilde{\varepsilon}_5)$	

Using three stacks, it turns out that there are solutions of the untwisted components of the $R-R$-tadpole equation for the most appealing given stack sizes $N_1 = 3, N_2 = 2, N_3 = 1$. After the construction of fractional cycles, it is observed that all existing solutions with chiral matter contain antisymmetric (and by this also symmetric) representations of the gauge group, but it is possible to have this only on the most "harmless" $N_3 = 1$-stack. Requiring this additional constraint, it is found that just three bifundamental representations between the U(3)- and the U(2)-stack are not possible, so one cannot obtain three left-handed quark generations.

If one turns over to 4 stacks, it is observed quickly from the untwisted components of the $R-R$-tadpole equation that the most favorable configuration $N_1 = 3$, $N_2 = 2$, $N_3 = 1$, $N_4 = 1$ does not produce any solutions. However, the two configurations $N_1 = 4$, $N_2 = 2$, $N_3 = 1$, $N_4 = 1$ and $N_1 = 3$, $N_2 = 2$, $N_3 = 2$, $N_4 = 1$, which still might be acceptable, provide for solutions. Requiring again no (anti-)symmetric representations on the first brane, it is observed that just on the **ABB**-torus, there exist solutions with three bifundamental representations between the first and the second brane, i.e., there exist three left-handed quarks. This seems rather nice, but in the further investigation of these models it turns out that there are always more than three U_R and D_R quarks in the $(\bar{\mathbf{3}}, 1)$ representation of $SU(3) \times SU(2)$ localized at intersections between the U(3) and any one of the U(1) stacks.

From all this, we have to conclude that there have to be at least five stacks of branes to obtain three quark generations and it indeed turns out that with this number of stacks, it is possible to obtain a very appealing class of phenomenological models which will be introduced in the following section.

B. 5 stack configurations

For the search of 5 stack models, we cannot proceed exactly in the same way as for 4 stack configurations, because it would require much too much computer power to got through all possible constructions with fractional cycles. Therefore, we will alter our approach in the following way: we fix the stack size on the first three stacks to be $N_a = 3$, $N_b = 2$ and $N_c = 1$. Then we require from the beginning that first, there are no (anti-)symmetric representations of the U(3) gauge factor, second, that the absolute value of intersection numbers are $|I_{ab} + I_{ab'}| \equiv 3$ and $|I_{ac} + I_{ac'}| \equiv 6$. This just means that we demand (up to conjugation) three left-handed quark generations in the bifundamental representation $(\mathbf{3}, \mathbf{2})$ and that the sum of U_R and D_R quark generations in the representation $(\bar{3}, 1)$ has to be six.

For all homological cycles fulfilling this condition, we now search for a variable stack size on the 4th and 5th torus if (and for which N_d, N_e) the two untwisted components of the $R-R$-tadpole equations can be fulfilled. For the remaining possibilities, we construct all possible fractional cycles also on the 4th and 5th stack and then look for the spectra which are possible. At this point, there is a rather miraculous observation we have made: if we furthermore require that there are no (anti-)symmetric representations of any gauge factor, there remains exactly *one* class of models with a given chiral spectrum.[6] This model has the two stack sizes $N_d = N_e = 1$. The same observation has been made on all three possible tori which give results at all (namely the **AAB**, **ABA**, and **ABB** tori) and the chiral spectra of these models all agree. Even more astonishingly, this model resembles almost exactly the nonsupersymmetric model of [20] with regard to the chiral spectrum. There is just one difference: on the 5th stack e, there are three additional bifundamental representations. At this point, we should make another remark, being that all nonvanishing intersection numbers have an absolute value 3, this seems to be a very aesthetical feature of this model and most likely could be understood in more depth directly from the $\mathbb{Z}_6$ symmetry.

There is another observation which completely agrees on the whole class of possibilities: the third and fifth homological cycles are $\Omega\mathcal{R}$-invariant. A detailed calculation shows that they both indeed are SO(2)-stacks. The chiral spectrum of this class of models is shown in Table X for an example on the **AAB** torus.

[6]This statement is valid up to an over-all minus sign of the intersection numbers, an exchange of the so-far equivalent 4th and 5th stack and an exchange between the general sectors xy and xy', all leading to the same massless spectrum. The same result was found in [20].

TABLE X. Chiral spectrum of the model class with gauge group $SU(3)_a \times SU(2)_b \times SO(2)_c \times U(1)_d \times SO(2)_e \times U(1)_a \times U(1)_b$.

Chiral spectrum of five stack models with $N_a = 3$, $N_b = 2$, $N_c = N_d = N_e = 1$						
	Sector	$SU(3)_a \times SU(2)_b \times SO(2)_c \times SO(2)_e$	Q_a	Q_b	Q_d	$\frac{1}{3}Q_a + Q_d$
Q_L	ab'	$3 \times (\bar{\mathbf{3}}, \mathbf{2}; 1, 1)$	-1	-1	0	$-\frac{1}{3}$
U_R, D_R	ac	$3 \times (\mathbf{3}, 1; \mathbf{2}, 1)$	1	0	0	$\frac{1}{3}$
L	bd'	$3 \times (1, \mathbf{2}; 1, 1)$	0	1	1	1
E_R, N_R	cd	$3 \times (1, 1; \mathbf{2}, 1)$	0	0	-1	-1
	be	$3 \times (1, \mathbf{2}; 1, \mathbf{2})$	0	1	0	0

The fact that we have two SO(2)- instead of U(1)-stacks is not a problem, because it just means that the two fractional branes coincide with their $\Omega\mathcal{R}$-mirror branes. In the nonchiral spectrum there is the adjoint representation of both gauge factors, being related to the unconstrained distance between the two branes and their mirrors on T_3^2. If one gives a vacuum expectation value (VEV) to these fields, then the branes and their mirrors are distinguishable and the gauge group is a U(1) instead of the SO(2) which indeed has the same rank. Then any bifundamental of the type $(\mathbf{3}, \mathbf{2})$, where the $\mathbf{3}$ comes for instance from a U(3) and the $\mathbf{2}$ from the SO(2), splits up into a $(\mathbf{3}, 1)$ and a $(\mathbf{3}, -1)$, where one and -1 now are the U(1)-charges. After this transition, the U_R- and D_R-quarks (and the E_R and N_R) are distinguishable as usual by their opposite U(1) charge.

Besides these common properties, the nonchiral spectrum which has been calculated according to the lines of Sec. III disagrees for different models on just one and also between different tori. This is well understandable, because it does not only depends on the homology, but also on the geometrical properties of the branes and the choice of the lattice. In the next section, we will discuss two different explicit examples of this class of models in more detail.

VI. THE SUPERSYMMETRIC STANDARD MODEL

In the previous section, we systematically explored how it is possible to obtain three quark generations in a stable and $R-R$-tadpole free D6-brane configuration. In this section, we explore in detail how the supersymmetric standard model arises.

TABLE XI. The setup of the D6-branes in the five stack model on the **AAB** torus.

	(n_I, m_I)	$(\sigma_1, \sigma_2, \sigma_3, \sigma_4)$	(τ_1, τ_2)	$\mathbb{Z}_2$
$N_a = 3$	$(-2, 1; -1, 2; -2, 1)$	(0, 0, 0, 0)	(0, 0)	$-$
$N_b = 2$	$(-1, 0; -1, 1; -1, 2)$	(0, 0, 0, 0)	(1, 0)	+
$N_c = 1$	$(-2, 1; -2, 1; -1, 2)$	(0, 0, 0, 0)	(1, 0)	+
$N_d = 1$	$(-1, 0; -1, 1; -1, 2)$	(0, 0, 0, 0)	(0, 0)	$-$
$N_e = 1$	$(-1, 1; -1, 1; -2, 1)$	(0, 0, 0, 0)	(0, 0)	$-$

A. The model on the AAB torus

The explicit configuration that shall be discussed in this section is given in Table XI, the homological cycles and intersection numbers are listed in Table XII. After the displacement of the third and fifth stack on the third 2-torus (as discussed in the preceding section), the chiral spectrum takes the form as shown in Table XIII. We can immediately calculate which U(1) factors remain massless after applying the Green-Schwarz mechanism which is discussed in detail in Sec. IV. The result is that one obtains three U(1)s which are free of triangle anomalies, being $Q_{B-L} = -\frac{1}{3}Q_a - Q_d$, Q_c and Q_e. As in similar constructions, the first one is the $B-L$ symmetry, Q_c is twice the third component of the right-handed weak isospin. Q_e is an additional U(1) symmetry under which none of the standard model particles transforms, only the two additional fields.

Also the linear combination

$$Q_Y = -\frac{1}{6}Q_a + \frac{1}{2}Q_c - \frac{1}{2}Q_d \qquad (49)$$

is massless, being the hypercharge Y. Every chiral field has the correct quantum numbers (for both hypercharge and $B-L$ symmetry), the only mystical one being the two additional kinds of fields at the be and be' intersections. Actually, these two kinds of fields have the right quantum numbers to be the supersymmetric standard model partners of the Higgs fields with a vanishing hypercharge, H and $\bar{H}$.[7] The only problem in the present construction is the fact that these bifundamental fields do not stretch from the second stack to the c-brane, but to the e-brane, and therefore do not give rise to the standard Yukawa couplings.

But the problem at first sight can be overcome as well. It is known that in many cases a gauge breaking where two

[7]The hypercharge could also be defined with an additional factor of $-1/2Q_e$, then the two additional kinds of fields would have the more familiar opposite hypercharge $-1/2$ and $1/2$.

TABLE XII. The homology cycles and intersection numbers (all other intersection numbers vanishing) of the D6-branes in the five stack model on the **AAB** torus.

Homology cycles	Intersections	
$\Pi_a = \frac{1}{2}(3\rho_1 + 3\rho_2 - \varepsilon_1 + 2\varepsilon_2 - \varepsilon_5 + 2\tilde{\varepsilon}_1 - \tilde{\varepsilon}_2 + 2\tilde{\varepsilon}_5)$	$I_{ab} = 0$	$I_{ab'} = -3$
$\Pi_b = \frac{1}{2}(\rho_1 + \rho_2 + \varepsilon_1 + 2\varepsilon_2 + \varepsilon_5 - 2\tilde{\varepsilon}_1 - \tilde{\varepsilon}_2 - 2\tilde{\varepsilon}_5)$	$I_{ac} = 3$	$I_{ac'} = 3$
$\Pi_c = \frac{1}{2}(3\rho_1 + 3\rho_2 + \varepsilon_1 - \varepsilon_2 + \varepsilon_3 + \tilde{\varepsilon}_1 - \tilde{\varepsilon}_2 + \tilde{\varepsilon}_3)$	$I_{bd} = 0$	$I_{bd'} = 3$
$\Pi_d = \frac{1}{2}(\rho_1 + \rho_2 + \varepsilon_1 - 2\varepsilon_2 + \varepsilon_5 - 2\tilde{\varepsilon}_1 + \tilde{\varepsilon}_2 - 2\tilde{\varepsilon}_5)$	$I_{cd} = 3$	$I_{cd'} = -3$
$\Pi_e = \frac{1}{2}(\rho_1 + \rho_2 - \varepsilon_1 - \varepsilon_2 - \varepsilon_3 - \tilde{\varepsilon}_1 - \tilde{\varepsilon}_2 - \tilde{\varepsilon}_3)$	$I_{be} = 3$	$I_{be'} = 3$

unitary gauge groups are broken to the diagonal subgroup is possible, in our case the breaking $U(1)_c \times U(1)_e \to U(1)_C$ would be needed. In the language of D-branes, this requires a brane recombination mechanism which in some cases can be understood in the effective field theory just as a Higgs effect. We will explain in the following why this is exactly the case for the present model.

If two stacks of D-branes preserve a common $\mathcal{N} = 2$ supersymmetry, then a massless hypermultiplet being localized at the intersection indicates that there is a possible deformation of the two stacks into just one recombined one. In our case, which is similar to the one described in [36], two factorizable branes can only preserve a common $\mathcal{N} = 2$ supersymmetry if they are parallel on one of the three tori. To understand this for our concrete model, we have to take a look at the nonchiral spectrum. This has been calculated for the concrete model of Table XI as described in Sec. III and the result is shown in Table XIV.

From Table XIV, we can immediately see that the necessary hypermultiplets are indeed existing, being the ones in the sector between the c and e-brane. If we take a closer look at the computation and for a moment distinguish between the different orbifold images under the θ action,[8] we observe that the two hypermultiplets are not in the ce sector, but in the $c(\theta^2 e)$ sector. In this sector, the branes c and $(\theta^2 e)$ are indeed parallel on the third torus, see Fig. 2. Therefore, we can recombine in this way the c with the $(\theta^2 e)$-brane [and at the same time the (θc) with the e brane and the $(\theta^2 c)$ with the (θe) brane] by giving a VEV to the two hypermultiplets in the following way: it is possible to understand the recombination as a Higgs effect in the $\mathcal{N} = 2$ effective theory, if there exists a flat direction $\langle h_1 \rangle = \langle h_2 \rangle$ in the D-term potential

$$V_D \sim \frac{1}{2g^2}(h_1\bar{h}_1 - h_2\bar{h}_2)^2, \qquad (50)$$

along which the gauge symmetry is broken to the diagonal subgroup. Here, h_1 and h_2 denote the two chiral multiplets inside the hypermultiplet. If one gauge factor is a U(1), there is a potential problem: if the two involved stacks intersect only once (meaning that there is just one hypermultiplet), then the D-flat direction is not F-flat because there is a superpotential, coupling the two chiral multiplets to the adjoint vector multiplet Φ as

$$W = h_1 h_2 \Phi. \qquad (51)$$

Therefore $\partial W/\partial\Phi$ imposes $h_1 h_2 = 0$, meaning that we cannot give a VEV to both fields h_1 and h_2 at the same time (what D-flatness actually requires).

The situation in our case is different: looking at the geometrical intersections of brane c and $(\theta^2 e)$ in Fig. 2, it can be observed that they intersect on both the first and the second torus twice, but hypermultiplets live only on two of the intersections, because the relative Wilson line on T_1^2 projects out the other two.

For two hypermultiplets, there is one flat direction which is obtained by combining the VEVs for h_1, h_2 in one hypermultiplet and for $\tilde{h}_1, \tilde{h}_2$ in the other, such that both the D- and F-flatness conditions are fulfilled. This means explicitly that

$$W_1 = h_1 h_2 \Phi, \qquad W_2 = \tilde{h}_1 \tilde{h}_2 \Phi. \qquad (52)$$

From F-flatness, it is possible to give h_2 and $\tilde{h}_1$ a nonvanishing VEV (while at the same time giving a vanishing one to h_1 and $\tilde{h}_2$) and still obtain a flat direction in the D-term potential because they couple to the same vector

[8] Of course, in the end we have to sum over all θ images such that the result is invariant under the orbifold action.

TABLE XIII. Chiral spectrum of the model class with gauge group $SU(3)_a \times SU(2)_b \times U(1)_a \times U(1)_b \times U(1)_c \times U(1)_d \times U(1)_e$.

Chiral spectrum of five stack model on **AAB** torus									
	Sector	$SU(3)_a \times SU(2)_b$	Q_a	Q_b	Q_c	Q_d	Q_e	Q_{B-L}	Q_Y
Q_L	ab'	$3 \times (\bar{\mathbf{3}}, \mathbf{2})$	−1	−1	0	0	0	$\frac{1}{3}$	$\frac{1}{6}$
U_R	ac	$3 \times (\mathbf{3}, 1)$	1	0	−1	0	0	$-\frac{1}{3}$	$-\frac{2}{3}$
D_R	ac'	$3 \times (\mathbf{3}, 1)$	1	0	1	0	0	$-\frac{1}{3}$	$\frac{1}{3}$
L	bd'	$3 \times (1, \mathbf{2})$	0	1	0	1	0	−1	$-\frac{1}{2}$
E_R	cd	$3 \times (1, 1)$	0	0	1	−1	0	1	1
N_R	cd'	$3 \times (1, 1)$	0	0	−1	−1	0	1	0
	be	$3 \times (1, \mathbf{2})$	0	1	0	0	−1	0	0
	be'	$3 \times (1, \mathbf{2})$	0	1	0	0	1	0	0

TABLE XIV. Nonchiral massless and light open spectrum of the model in Table XI on **AAB** computed from 3-cycles. If the factorizable cycles are parallel on T_3^2, the mass of the states is proportional to the relative distance $\Sigma_{xy} = |\sigma_{56}^x - \sigma_{56}^y|$ of the D6-branes on this torus, $\sqrt{\alpha'} m_{xy} = \Sigma_{xy}$. The distance has to be taken to be in the range $\Sigma_{xy} \in [0, 1/2] \times R_3$ with R_3 being the (dimensionless) length scale on T_3^2. σ_{56}^x denotes the distance of brane x from the origin on T_3^2. The $\mathbf{3}_A$ of $U(3)_a$ transforms as $\mathbf{3}_2$ under the decomposition $U(3)a \to SU(3)_a \times U(1)_a$, while the $\bar{\mathbf{2}}$ of $U(2)_b$ decomposes into $\mathbf{2}_{-1}$ of $SU(2)_b \times U(1)_b$. The physical U(1) charges can be computed from Sec. IV.

Nonchiral massless and light open spectrum, **AAB** on $T^6/(\mathbb{Z}_6 \times \Omega\mathcal{R})$					
Sector	$U(3)_a \times U(2)_{b(Q_c,Q_d,Q_e)}$	$\sqrt{\alpha'}m$	Sector	$U(3)_a \times U(2)_{b(Q_c,Q_d,Q_e)}$	$\sqrt{\alpha'}m$
aa	$16 \times (\mathbf{9}, 1)_{0,0,0}$	0	ad'	$6 \times [(\mathbf{3}, 1)_{0,1,0} + h.c.]$	0
bb	$4 \times (1, \mathbf{4})_{0,0,0}$	0		$(\mathbf{3}, 1)_{0,1,0} + h.c.$	$\Sigma_{ad'}$
cc	$16 \times (1, 1)_{0,0,0}$	0	ae	$6 \times [(\mathbf{3}, 1)_{0,0,-1} + h.c.]$	0
dd	$4 \times (1, 1)_{0,0,0}$	0		$(\mathbf{3}, 1)_{0,0,-1} + h.c.$	Σ_{ae}
ee	$4 \times (1, 1)_{0,0,0}$	0	ae'	$6 \times [(\mathbf{3}, 1)_{0,0,1} + h.c.]$	0
aa'	$9 \times [(\mathbf{3}_A, 1)_{0,0,0} + h.c.]$	0		$(\mathbf{3}, 1)_{0,0,1} + h.c.$	$\Sigma_{ae'}$
	$5 \times [(\mathbf{3}_A, 1)_{0,0,0} + h.c.]$	$\Sigma_{aa'}$	bc	$6 \times [(1, \mathbf{2})_{-1,0,0} + h.c.]$	0
bb'	$3 \times [(1, \mathbf{1}_A)_{0,0,0} + h.c.]$	0		$(1, \mathbf{2})_{-1,0,0} + h.c.$	Σ_{bc}
	$(1, \mathbf{1}_A)_{0,0,0} + h.c.$	$\Sigma_{bb'}$	bc'	$6 \times [(1, \mathbf{2})_{1,0,0} + h.c.]$	0
ab	$2 \times [(\mathbf{3}, \bar{\mathbf{2}})_{0,0,0} + h.c.]$	Σ_{ab}		$(1, \mathbf{2})_{1,0,0} + h.c.$	$\Sigma_{bc'}$
ac	$3 \times [(\mathbf{3}, 1)_{-1,0,0} + h.c.]$	0	ce	$2 \times [(1, 1)_{1,0,-1} + h.c.]$	Σ_{ce}
	$4 \times [(\mathbf{3}, 1)_{-1,0,0} + h.c.]$	Σ_{ac}	ce'	$2 \times [(1, 1)_{1,0,1} + h.c.]$	$\Sigma_{ce'}$
ac'	$3 \times [(\mathbf{3}, 1)_{1,0,0} + h.c.]$	0	de	$3 \times [(1, 1)_{0,1,-1} + h.c]$	0
	$4 \times [(\mathbf{3}, 1)_{1,0,0} + h.c.]$	$\Sigma_{ac'}$		$(1, 1)_{0,1,-1} + h.c$	Σ_{de}
ad	$3 \times [(\mathbf{3}, 1)_{0,-1,0} + h.c.]$	0	de'	$3 \times [(1, 1)_{0,1,1} + h.c]$	0
	$4 \times [(\mathbf{3}, 1)_{0,-1,0} + h.c.]$	Σ_{ad}		$(1, 1)_{0,1,1} + h.c$	$\Sigma_{de'}$

multiplet Φ, i.e., the D-term looks like

$$V_D \sim \frac{1}{2g^2}(h_1\bar{h}_1 - h_2\bar{h}_2 + \tilde{h}_1\bar{\tilde{h}}_1 - \tilde{h}_2\bar{\tilde{h}}_2)^2. \tag{53}$$

The D-term and F-terms are indeed flat for the choice

$$\langle h_1 \rangle = \langle \tilde{h}_2 \rangle = 0, \tag{54}$$

$$\langle h_2 \rangle = \langle \tilde{h}_1 \rangle \neq 0. \tag{55}$$

This construction is just possible if the VEVs that we have given to the fields in between the c and c' brane and the e and e' brane (formerly the adjoints on the world volume of the $\Omega\mathcal{R}$ invariant stacks, in order to get U(1) instead of SO(2) gauge groups) are the same, but this is completely unproblematic.

Homologically, we only have to add the two cycles Π_c and Π_e to get the recombined brane, which shall be denoted as $\Pi_C = \Pi_c + \Pi_e$. This complex cycle has the same volume as the sum of volumes of the two cycles before recombination occurs. The intersection numbers of the recombined cycles are given in Table XV. The final chiral spectrum after the recombination is given in Table XVI. The massless U(1)s can be checked again using the computation of the Green-Schwarz couplings along the lines of Sec. IV. There are two nonanomalous U(1)s, being $Q_{B-L} = -\frac{1}{3}Q_a - Q_d$ and Q_C. Fortunately, the hypercharge

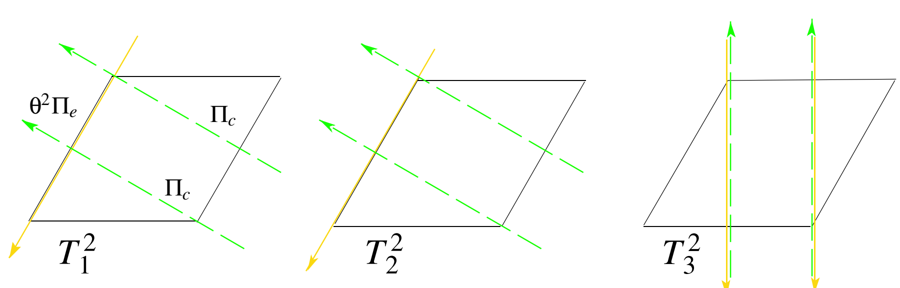

FIG. 2 (color online). Geometrical intersections of branes c and $(\theta^2 e)$ on the **AAB** torus. The gauge group is $U(1)_c \times U(1)_e$ if the branes are displaced from the origin on T_3^2. Remember that the $\mathcal{R}$ invariant plane lies along $\pi_1 \otimes \pi_3 \otimes (\pi_5 + \pi_6)$ with the notation as in Fig. 1.

TABLE XV. The intersection numbers (all other intersection numbers vanishing) of the D6-branes in the final 5 stack model on the **AAB** torus.

Intersections	
$I_{ab} = 0$	$I_{ab'} = -3$
$I_{aC} = 3$	$I_{aC'} = 3$
$I_{bd} = 0$	$I_{bd'} = 3$
$I_{Cd} = 3$	$I_{Cd'} = -3$
$I_{bC} = 3$	$I_{bC'} = 3$

$$Q_Y = -\frac{1}{6}Q_a + \frac{1}{2}Q_C - \frac{1}{2}Q_d \tag{56}$$

is still massless and the two types of fields H and $\bar{H}$ have just the opposite hypercharge $-1/2$ and $1/2$. Therefore, they can be exactly understood as the superpartners of the standard model Higgs with a definite chirality.

B. The model on the ABA torus

The explicit configuration that shall be discussed in this section is given in Table XVII, the homological cycles and intersection numbers are listed in Table XVIII.

Comparing Table XVII with the model of the preceding section, Table XI, reveals that the realization on the torus is very different, for instance in the previous case stacks b and d are parallel while in this model stacks a, b, and d are parallel as well as c and e. Furthermore, the stacks c and e are displaced from the origin on T_1^2.

Nevertheless, the chiral spectrum agrees up to a conjugation with the chiral spectrum of the model on the **AAB** torus, see Table XIII. The massless U(1)s after the application of the Green-Schwarz formalism do also completely agree. On the other hand, calculating the nonchiral spectrum for this second explicit model shows that it is indeed very different as compared to the one on the torus. The spectrum is listed in Table XIX. Remarkably, the brane recombination mechanism which has been described in the last section does not work for this model: the hypermultiplets in the sector between the c and the e brane are absent due to the relative Wilson line on T_2^2.

Therefore, we can draw the conclusion that it is only possible for a subclass of models with the same initial chiral spectrum to break it to the exact supersymmetric standard model.

TABLE XVI. Chiral spectrum of the model class with gauge group $SU(3)_a \times SU(2)_b \times U(1)_a \times U(1)_b \times U(1)_C \times U(1)_d$.

Chiral spectrum of 5 stack model on **AAB** torus							
	Sector	$SU(3)_a \times SU(2)_b$	Q_a	Q_b	Q_C	Q_d	Q_Y
Q_L	ab'	$3 \times (\bar{\mathbf{3}}, \mathbf{2})$	-1	-1	0	0	$\frac{1}{6}$
U_R	aC	$3 \times (\mathbf{3}, 1)$	1	0	-1	0	$-\frac{2}{3}$
D_R	aC'	$3 \times (\mathbf{3}, 1)$	1	0	1	0	$\frac{1}{3}$
L	bd'	$3 \times (1, \mathbf{2})$	0	1	0	1	$-\frac{1}{2}$
E_R	Cd	$3 \times (1, 1)$	0	0	1	-1	1
N_R	Cd'	$3 \times (1, 1)$	0	0	-1	-1	0
H	bC	$3 \times (1, \mathbf{2})$	0	1	-1	0	$-\frac{1}{2}$
$\bar{H}$	bC'	$3 \times (1, \mathbf{2})$	0	1	1	0	$\frac{1}{2}$

VII. LEFT-RIGHT SYMMETRIC MODELS

In order to obtain a left-right symmetric model with three quark generations, also at least five stacks are required. For the lattices **AAA**, **BBA**, and **BBB**, it turns out that all brane configurations with $SU(3)_a \times SU(2)_b \times SU(2)_c$, no (anti)symmetric chiral states of $SU(3)_a$, i.e, $\Pi_a \circ \Pi_{a'} = 0$, and three left and right-handed quark generations, i.e., $3 \times (\mathbf{3}_a, \mathbf{2}_b) + 3 \times (\bar{\mathbf{3}}_a, \mathbf{2}_c)$ in the chiral spectrum, wrap larger bulk cycles than the O6-planes. Therefore, no supersymmetric chiral left-right symmetric 3-generation model on these tori fulfills $R-R$-tadpole cancellation. This result agrees completely with the observation made for the ansatz $N_a = 3$, $N_b = 2$ and $N_c = 1$ in the previous section. For the **ABA** and **ABB** lattices, the minimal requirement on three stacks of fractional D6-branes can be fulfilled. However, the twisted $R-R$ charges cannot be canceled by any configuration with at most five stacks of D6-branes—at least if we require that the two additional gauge groups have at most rank two.

For the lattice **AAB**, there exists chiral 3-generation left-right symmetric models with five stacks. Two distinct chiral spectra occur, one of them containing (anti)symmetric representations of some SU(2) factors. The other chiral spectrum encloses only bifundamental representations as displayed in Table XX. The gauge group of the standard model part consists of $SU(3)_a \times SU(2)_b \times SU(2)_c \times U(1)_d$. In order to fulfill tadpole cancellation, an additional stack with gauge group $U(2)_e$ is required. Apart from the left/right symmetric MSSM particles, two kinds of exotic chiral particles charged under the additional $U(2)_e$ arise. These seemingly unwanted exotic particles, however, have the correct quantum numbers to combine into composite Higgs particles, i.e., also in the left/right symmetric models the Higgs fields can originate from the chiral spectrum due to an "internal" $U(2)_e$ symmetry.

TABLE XVII. The setup of the D6-branes in the 5 stack model on the **ABA** torus.

	(n_I, m_I)	$(\sigma_1, \sigma_2, \sigma_3, \sigma_4)$	(τ_1, τ_2)	$\mathbb{Z}_2$
$N_a = 3$	$(-1, 1; -1, 1; -2, 1)$	$(0, 0, 0, 0)$	$(0, 0)$	$-$
$N_b = 2$	$(-1, 1; -1, 1; -2, 1)$	$(0, 0, 0, 0)$	$(0, 1)$	$-$
$N_c = 1$	$(-1, 0; -1, 1; -1, 2)$	$(0, \frac{1}{2}, 0, 0)$	$(1, 0)$	$-$
$N_d = 1$	$(-1, 1; -1, 1; -2, 1)$	$(0, 0, 0, 0)$	$(0, 0)$	$+$
$N_e = 1$	$(-1, 0; -1, 1; -1, 2)$	$(0, \frac{1}{2}, 0, 0)$	$(1, 1)$	$-$

TABLE XVIII. The homology cycles and intersection numbers (all other intersection numbers vanishing) of the D6-branes in the 5 stack model on the **ABA** torus.

Homology cycles	Intersections	
$\Pi_a = \frac{1}{2}(\rho_1 + \rho_2 - \varepsilon_1 - \varepsilon_2 - \varepsilon_3 - \tilde{\varepsilon}_1 - \tilde{\varepsilon}_2 - \tilde{\varepsilon}_3)$	$I_{ab} = 0$	$I_{ab'} = 3$
$\Pi_b = \frac{1}{2}(\rho_1 + \rho_2 - \varepsilon_1 + \varepsilon_2 + \varepsilon_3 - \tilde{\varepsilon}_1 + \tilde{\varepsilon}_2 + \tilde{\varepsilon}_3)$	$I_{ac} = -3$	$I_{ac'} = -3$
$\Pi_c = \frac{1}{2}(\rho_1 + \rho_2 + 3\varepsilon_1 + 2\varepsilon_3 + \varepsilon_4 - \tilde{\varepsilon}_3 + \tilde{\varepsilon}_4)$	$I_{bd} = 0$	$I_{bd'} = -3$
$\Pi_d = \frac{1}{2}(\rho_1 + \rho_2 + \varepsilon_1 + \varepsilon_2 + \varepsilon_3 + \tilde{\varepsilon}_1 + \tilde{\varepsilon}_2 + \tilde{\varepsilon}_3)$	$I_{cd} = -3$	$I_{cd'} = 3$
$\Pi_e = \frac{1}{2}(\rho_1 + \rho_2 + 3\varepsilon_1 - 2\varepsilon_3 - \varepsilon_4 + \tilde{\varepsilon}_3 - \tilde{\varepsilon}_4)$	$I_{be} = -3$	$I_{be'} = -3$

TABLE XIX. Nonchiral massless and light open spectrum of the model from Table XVII on the **ABA** torus. The notation agrees with Table XIV.

Nonchiral massless and light open spectrum, **ABA** on $T^6/(\mathbb{Z}_6 \times \Omega\mathcal{R})$					
Sector	$U(3)_a \times U(2)_{b(Q_c,Q_d,Q_e)}$	$\sqrt{\alpha'}m$	Sector	$U(3)_a \times U(2)_{b(Q_c,Q_d,Q_e)}$	$\sqrt{\alpha'}m$
aa	$4 \times (\mathbf{9}, 1)_{0,0,0}$	0	ab	$3 \times [(\mathbf{3}, \bar{\mathbf{2}})_{0,0,0} + h.c.]$	0
bb	$4 \times (1, \mathbf{4})_{0,0,0}$	0	ab'	$(\mathbf{3}, \mathbf{2})_{0,0,0} + h.c.$	$\Sigma_{ab'}$
cc	$4 \times (1, 1)_{0,0,0}$	0	ac	$(\mathbf{3}, 1)_{-1,0,0} + h.c.$	Σ_{ac}
dd	$4 \times (1, 1)_{0,0,0}$	0	ac'	$(\mathbf{3}, 1)_{1,0,0} + h.c.$	$\Sigma_{ac'}$
ee	$4 \times (1, 1)_{0,0,0}$	0	ad	$2 \times [(\mathbf{3}, 1)_{0,-1,0} + h.c.]$	Σ_{ad}
aa'	$(2 \times \mathbf{3}_A + \mathbf{6}_S, 1)_{0,0,0} + h.c.$	0	ad'	$3 \times [(\mathbf{3}, 1)_{0,1,0} + h.c.]$	0
	$(\mathbf{3}_A, 1)_{0,0,0} + h.c.$	$\Sigma_{aa'}$	ae	$(\mathbf{3}, 1)_{0,0,-1} + h.c.$	Σ_{ae}
bb'	$(1, 2 \times \mathbf{1}_A + \mathbf{3}_S)_{0,0,0} + h.c.$	0	ae'	$(\mathbf{3}, 1)_{0,0,1} + h.c.$	$\Sigma_{ae'}$
	$(1, \mathbf{1}_A)_{0,0,0} + h.c.$	$\Sigma_{bb'}$	bc	$(1, \mathbf{2})_{-1,0,0} + h.c.$	Σ_{bc}
cc'	$(1, 1)_{2,0,0} + h.c.$	0	bc'	$(1, \mathbf{2})_{1,0,0} + h.c.$	$\Sigma_{bc'}$
dd'	$(1, 1)_{0,2,0} + h.c.$	0	be	$(1, \mathbf{2})_{0,0,-1} + h.c.$	Σ_{be}
ee'	$(1, 1)_{0,0,2} + h.c.$	0	be'	$(1, \mathbf{2})_{0,0,1} + h.c.$	$\Sigma_{be'}$

TABLE XX. Chiral spectrum of a left-right symmetric model. In the last two columns, the charges under the two massless linear combinations for the specific D6-brane configuration (Table XXI) are displayed.

Chiral left-right symmetric spectrum of an **AAB** model on $T^6/(\mathbb{Z}_6 \times \Omega\mathcal{R})$									
	Sector	$SU(3)_a \times SU(2)_b \times SU(2)_c \times SU(2)_e$	Q_a	Q_b	Q_c	Q_d	Q_e	Q_{B-L}	$\tilde{Q}$
Q_L	ab'	$3 \times (\mathbf{3}, \mathbf{2}, 1; 1)$	1	1	0	0	0	1/3	2
U_R, D_R	ac'	$3 \times (\bar{\mathbf{3}}, 1, \mathbf{2}; 1)$	−1	0	−1	0	0	−1/3	−2
L	bd'	$3 \times (1, \mathbf{2}, 1; 1)$	0	−1	0	−1	0	−1	-1
E_R, N_R	cd'	$3 \times (1, 1, \mathbf{2}; 1)$	0	0	1	1	0	1	1
	be'	$3 \times (1, \mathbf{2}, 1; \mathbf{2})$	0	−1	0	0	−1	0	−5/2
	ce'	$3 \times (1, 1, \mathbf{2}; \mathbf{2})$	0	0	1	0	1	0	5/2

TABLE XXI. The setup of the D6-branes in the five stack left/right symmetric model on the **AAB** torus.

	(n_I, m_I)	$(\sigma_1, \sigma_2, \sigma_3, \sigma_4)$	(τ_1, τ_2)	$\mathbb{Z}_2(= \tau_0)$
$N_a = 3$	$(-2, 1; -1, 2; -2, 1)$	$(0, 0, 0, 0)$	$(0, 0)$	−
$N_b = 2$	$(-1, 0; -1, 1; -1, 2)$	$(0, 0, 0, 0)$	$(0, 1)$	+
$N_c = 2$	$(-1, 0; -1, 1; -1, 2)$	$(0, 0, 0, 0)$	$(1, 0)$	+
$N_d = 1$	$(-1, 0; -1, 1; -1, 2)$	$(0, 0, 0, 0)$	$(0, 0)$	−
$N_e = 2$	$(-1, 0; -1, 1; -1, 2)$	$(0, 0, 0, 0)$	$(1, 1)$	+

TABLE XXII. Nonchiral massless and light open spectrum of the left/right symmetric model computed from cycles.

Nonchiral left-right massless and light open spectrum, $\mathbf{AAB}$, $T^6/(\mathbb{Z}_6 \times \Omega\mathcal{R})$			
Sector	$U(3)_a \times U(2)_b \times U(2)_c \times U(2)_e (\times U(1)_d)$	Sector	$U(3)_a \times U(2)_b \times U(2)_c \times U(2)_e (\times U(1)_d)$
aa	$16 \times (\mathbf{9}, 1, 1; 1)_0$	ad	$7 \times [(\mathbf{3}, 1, 1; 1)_{-1} + h.c.]$
bb	$4 \times (1, \mathbf{4}, 1; 1)_0$	ad'	$7 \times [(\mathbf{3}, 1, 1; 1)_1 + h.c.]$
cc	$4 \times (1, 1, \mathbf{4}; 1)_0$	ae	$2 \times [(\mathbf{3}, 1, 1; \overline{\mathbf{2}})_0 + h.c.]$
dd	$4 \times (1, 1, 1; 1)_0$	ae'	$3 \times [(\mathbf{3}, 1, 1; \mathbf{2})_0 + h.c.]$
ee	$4 \times (1, 1, 1; \mathbf{4})_0$	bc	$3 \times [(1, \mathbf{2}, \overline{\mathbf{2}}; 1)_0 + h.c.]$
aa'	$14 \times [(\mathbf{3}_A, 1, 1; 1)_0 + h.c.]$	bc'	$3 \times [(1, \mathbf{2}, \mathbf{2}; 1)_0 + h.c.]$
bb'	$4 \times [(1, \mathbf{1}_A, 1; 1)_0 + h.c.]$	be	$3 \times [(1, \mathbf{2}, 1; \overline{\mathbf{2}})_0 + h.c.]$
cc'	$4 \times [(1, 1, \mathbf{1}_A; 1)_0 + h.c.]$	be'	$(1, \mathbf{2}, 1; \mathbf{2})_0 + h.c.$
ee'	$4 \times [(1, 1, 1; \mathbf{1}_A)_0 + h.c.]$	ce	$3 \times [(1, 1, \mathbf{2}; \overline{\mathbf{2}})_0 + h.c.]$
ab	$2 \times [(\mathbf{3}, \overline{\mathbf{2}}, 1; 1)_0 + h.c.]$	ce'	$(1, 1, \mathbf{2}; \mathbf{2})_0 + h.c.$
ac	$2 \times [(\mathbf{3}, 1, \overline{\mathbf{2}}; 1)_0 + h.c.]$		

A concrete realization of this chiral spectrum is given in Table XXI. The corresponding 3-cycles can be read off from Tables XXIII and XXIV. Two Abelian gauge factors remain massless,

$$\begin{aligned} Q_{B-L} &= \frac{1}{3} Q_a + Q_d, \\ \tilde{Q} &= \frac{1}{4}(3Q_a + 5Q_b + 5Q_c - Q_d + 5Q_e). \end{aligned} \tag{57}$$

The nonchiral massless spectrum of the configuration XXI is listed in Table XXII.

VIII. CONCLUSIONS AND PROSPECTS

In this article, we have worked out all technical details of computing chiral and nonchiral massless spectra for intersecting fractional D6-branes on the $\mathbb{Z}_6$ orientifold. Discrete Wilson lines and distances of branes naturally occur due to the existence of exceptional cycles. The $\mathbb{Z}_3$ subsymmetry on each two torus freezes all complex structure moduli. Supersymmetry projects onto one out of two possible toroidal cycles. In addition, the D6-branes can wrap some of the ten existing exceptional 3-cycles. This leads to a $\mathcal{N} = 2$ supersymmetric gauge sector as compared to the $\mathcal{N} = 4$ ones for toroidal and orbifold backgrounds without exceptional 3-cycles. In a supersymmetric setup, all contributions to the bulk cycles are proportional to those of the O6-planes. In the $\mathbb{Z}_6$ orientifold, therefore, nontrivial intersections arise purely from the exceptional part of fractional branes. This approach also could be generalized to the two further symmetric orbifold groups $\mathbb{Z}_6 \times \mathbb{Z}_3$ and $\mathbb{Z}_{6'}$. The former is briefly mentioned in Appendix D, but does not seem to be of any phenomenological interest due to the small number of fractional cycles.

Already for 2-stack configurations, nontrivial chiral spectra with bifundamental representations exist. By systematically examining the possible 2, 3, and 4-stack configurations, we find that they cannot provide for nontrivial chiral spectra with the standard model gauge group. In all models, $R - R$ tadpoles are cancelled and supersymmetry is preserved globally, ensuring also the absence of $NS - NS$ tadpoles.

The first configurations with the standard model gauge group and also the correct chiral matter exist for five stacks. The most miraculous fact is that with only making the requirements of having at least one 3-, one 2- and one 1-stack of branes, having three quark generations, no chiral matter in antisymmetric representations, and preserving globally $\mathcal{N} = 1$ supersymmetry, there remains only *one* model with a definite chiral spectrum, which is shown in Table XIII.

Looking more closely at this model, it is not just very aesthetical in having only nonvanishing intersection numbers of an absolute value of 3, besides a massless hypercharge, it also seems to give rise to exactly the standard model particles in the chiral spectrum in addition to two additional kinds of particles in the bifundamental representation $(1, \mathbf{2})$ of $U(1) \times U(2)$. This looks like the two superpartners of the Higgs in a supersymmetric standard model, the only seemingly problem being the fact that the U(1) is not from the right stack, so at first sight they cannot give rise to the standard Yukawa couplings.

The nonchiral spectrum is rather different for two representatives of the discussed class of models. However, through a well motivated brane recombination process which is shown to exactly correspond to a Higgs branch in the effective $\mathcal{N} = 2$ theory of the type $U(1) \times U(1) \rightarrow U(1)$, these particles indeed can be identified with the two kinds of Higgs multiplets in one concrete realization. In homology, this process just means that we add the two factorizable 3-cycles for the two involved U(1)-branes to get the recombined one, which then is nonfactorizable. In the second presented example, the recombination still works in homology, but cannot be understood as a Higgs effect in the effective field theory,

TABLE XXIII. Relation between fixed points and wrapping numbers on $T_1^2 \times T_2^2$. The fixed point e_{11} does not give rise to any exceptional cycle. The bulk 2-cycle specified by the wrapping numbers can be displaced from the origin by $\sum_{i=1}^{4} \sigma_i \pi_i$ with $\sigma_i \in \{0, 1/2\}$.

Wrapping numbers intersecting fixed points for $T^6/\mathbb{Z}_6$						
(n_2, m_2) (n_1, m_1)	(Odd, even)	(Even, odd) $\sigma_3 = \sigma_4 = 0$	(Odd, odd)	(Odd, even)	(Even, odd) $\sigma_3 = \frac{1}{2}, \sigma_4 = 0$	(Odd, odd)
			$\sigma_1 = \sigma_2 = 0$			
(Odd, even)	$(e_{11})e_{14}e_{41}e_{44}$	$(e_{11})e_{15}e_{41}e_{45}$	$(e_{11})e_{16}e_{41}e_{46}$	$(e_{11})e_{14}e_{41}e_{44}$	$e_{14}e_{16}e_{44}e_{46}$	$e_{14}e_{15}e_{44}e_{45}$
(Even, odd)	$(e_{11})e_{14}e_{51}e_{54}$	$(e_{11})e_{15}e_{51}e_{55}$	$(e_{11})e_{16}e_{51}e_{56}$	$(e_{11})e_{14}e_{51}e_{54}$	$e_{14}e_{16}e_{54}e_{56}$	$e_{14}e_{15}e_{54}e_{55}$
(Odd, odd)	$(e_{11})e_{14}e_{61}e_{64}$	$(e_{11})e_{15}e_{61}e_{65}$	$(e_{11})e_{16}e_{61}e_{66}$	$(e_{11})e_{14}e_{61}e_{64}$	$e_{14}e_{16}e_{64}e_{66}$	$e_{14}e_{15}e_{64}e_{65}$
			$\sigma_1 = \frac{1}{2}, \sigma_2 = 0$			
(Odd, even)	$(e_{11})e_{14}e_{41}e_{44}$	$(e_{11})e_{15}e_{41}e_{45}$	$(e_{11})e_{16}e_{41}e_{46}$	$(e_{11})e_{14}e_{41}e_{44}$	$e_{14}e_{16}e_{44}e_{46}$	$e_{14}e_{15}e_{44}e_{45}$
(Even, odd)	$e_{61}e_{64}e_{41}e_{44}$	$e_{61}e_{65}e_{41}e_{45}$	$e_{61}e_{66}e_{41}e_{46}$	$e_{61}e_{64}e_{41}e_{44}$	$e_{64}e_{66}e_{44}e_{46}$	$e_{64}e_{65}e_{44}e_{45}$
(Odd, odd)	$e_{51}e_{54}e_{41}e_{44}$	$e_{51}e_{55}e_{41}e_{45}$	$e_{51}e_{56}e_{41}e_{46}$	$e_{51}e_{54}e_{41}e_{44}$	$e_{54}e_{56}e_{44}e_{46}$	$e_{54}e_{55}e_{44}e_{45}$
			$\sigma_1 = 0, \sigma_2 = \frac{1}{2}$			
(Odd, even)	$e_{61}e_{64}e_{51}e_{54}$	$e_{61}e_{65}e_{51}e_{55}$	$e_{61}e_{66}e_{51}e_{56}$	$e_{61}e_{64}e_{51}e_{54}$	$e_{64}e_{66}e_{54}e_{56}$	$e_{64}e_{65}e_{54}e_{55}$
(Even, odd)	$(e_{11})e_{14}e_{51}e_{54}$	$(e_{11})e_{15}e_{51}e_{55}$	$(e_{11})e_{16}e_{51}e_{56}$	$(e_{11})e_{14}e_{51}e_{54}$	$e_{14}e_{16}e_{54}e_{56}$	$e_{14}e_{15}e_{54}e_{55}$
(Odd, odd)	$e_{41}e_{44}e_{51}e_{54}$	$e_{41}e_{45}e_{51}e_{55}$	$e_{41}e_{46}e_{51}e_{56}$	$e_{41}e_{44}e_{51}e_{54}$	$e_{44}e_{46}e_{54}e_{56}$	$e_{44}e_{45}e_{54}e_{55}$
			$\sigma_1 = \sigma_2 = \frac{1}{2}$			
(Odd, even)	$e_{61}e_{64}e_{51}e_{54}$	$e_{61}e_{65}e_{51}e_{55}$	$e_{61}e_{66}e_{51}e_{56}$	$e_{61}e_{64}e_{51}e_{54}$	$e_{64}e_{66}e_{54}e_{56}$	$e_{64}e_{65}e_{54}e_{55}$
(Even, odd)	$e_{41}e_{44}e_{61}e_{64}$	$e_{41}e_{45}e_{61}e_{65}$	$e_{41}e_{46}e_{61}e_{66}$	$e_{41}e_{44}e_{61}e_{64}$	$e_{44}e_{46}e_{64}e_{66}$	$e_{44}e_{45}e_{64}e_{65}$
(Odd, odd)	$(e_{11})e_{14}e_{61}e_{64}$	$(e_{11})e_{15}e_{61}e_{65}$	$(e_{11})e_{16}e_{61}e_{66}$	$(e_{11})e_{14}e_{61}e_{64}$	$e_{14}e_{16}e_{64}e_{66}$	$e_{14}e_{15}e_{64}e_{65}$
		$\sigma_3 = 0, \sigma_4 = \frac{1}{2}$			$\sigma_3 = \sigma_4 = \frac{1}{2}$	
			$\sigma_1 = \sigma_2 = 0$			
(Odd ,even)	$e_{15}e_{16}e_{45}e_{46}$	$(e_{11})e_{15}e_{41}e_{45}$	$e_{15}e_{14}e_{44}e_{45}$	$e_{15}e_{16}e_{45}e_{46}$	$e_{14}e_{16}e_{44}e_{46}$	$(e_{11})e_{16}e_{41}e_{46}$
(Even, odd)	$e_{15}e_{16}e_{55}e_{56}$	$(e_{11})e_{15}e_{51}e_{55}$	$e_{14}e_{15}e_{54}e_{55}$	$e_{15}e_{16}e_{55}e_{56}$	$e_{14}e_{16}e_{54}e_{56}$	$(e_{11})e_{16}e_{51}e_{56}$
(Odd, odd)	$e_{15}e_{16}e_{65}e_{66}$	$(e_{11})e_{15}e_{61}e_{65}$	$e_{14}e_{15}e_{64}e_{65}$	$e_{15}e_{16}e_{65}e_{66}$	$e_{14}e_{16}e_{64}e_{66}$	$(e_{11})e_{16}e_{61}e_{66}$
			$\sigma_1 = \frac{1}{2}, \sigma_2 = 0$			
(Odd, even)	$e_{15}e_{16}e_{45}e_{46}$	$(e_{11})e_{15}e_{41}e_{45}$	$e_{14}e_{15}e_{44}e_{45}$	$e_{15}e_{16}e_{45}e_{46}$	$e_{14}e_{16}e_{44}e_{46}$	$(e_{11})e_{16}e_{41}e_{46}$
(Even, odd)	$e_{65}e_{66}e_{45}e_{46}$	$e_{61}e_{65}e_{41}e_{45}$	$e_{64}e_{65}e_{44}e_{45}$	$e_{65}e_{66}e_{45}e_{46}$	$e_{64}e_{66}e_{44}e_{46}$	$e_{61}e_{66}e_{41}e_{46}$
(Odd, odd)	$e_{55}e_{56}e_{45}e_{46}$	$e_{51}e_{55}e_{41}e_{45}$	$e_{54}e_{55}e_{44}e_{45}$	$e_{55}e_{56}e_{45}e_{46}$	$e_{54}e_{56}e_{44}e_{46}$	$e_{51}e_{56}e_{41}e_{46}$
			$\sigma_1 = 0, \sigma_2 = \frac{1}{2}$			
(Odd, even)	$e_{65}e_{66}e_{55}e_{56}$	$e_{61}e_{65}e_{51}e_{55}$	$e_{64}e_{65}e_{54}e_{55}$	$e_{65}e_{66}e_{55}e_{56}$	$e_{64}e_{66}e_{54}e_{56}$	$e_{61}e_{66}e_{51}e_{56}$
(Even, odd)	$e_{15}e_{16}e_{55}e_{56}$	$(e_{11})e_{15}e_{51}e_{55}$	$e_{14}e_{15}e_{54}e_{55}$	$e_{15}e_{16}e_{55}e_{56}$	$e_{14}e_{16}e_{54}e_{56}$	$(e_{11})e_{16}e_{51}e_{56}$
(Odd, odd)	$e_{45}e_{46}e_{55}e_{56}$	$e_{41}e_{45}e_{51}e_{55}$	$e_{44}e_{45}e_{54}e_{55}$	$e_{45}e_{46}e_{55}e_{56}$	$e_{44}e_{46}e_{54}e_{56}$	$e_{41}e_{46}e_{51}e_{56}$
			$\sigma_1 = \sigma_2 = \frac{1}{2}$			
(Odd, even)	$e_{65}e_{66}e_{55}e_{56}$	$e_{61}e_{65}e_{51}e_{55}$	$e_{64}e_{65}e_{54}e_{55}$	$e_{65}e_{66}e_{55}e_{56}$	$e_{64}e_{66}e_{54}e_{56}$	$e_{61}e_{66}e_{51}e_{56}$
(Even, odd)	$e_{45}e_{46}e_{65}e_{66}$	$e_{41}e_{45}e_{61}e_{65}$	$e_{44}e_{45}e_{64}e_{65}$	$e_{45}e_{46}e_{65}e_{66}$	$e_{44}e_{46}e_{64}e_{66}$	$e_{41}e_{46}e_{61}e_{66}$
(Odd, odd)	$e_{15}e_{16}e_{65}e_{66}$	$(e_{11})e_{15}e_{61}e_{65}$	$e_{14}e_{15}e_{64}e_{65}$	$e_{15}e_{16}e_{65}e_{66}$	$e_{14}e_{16}e_{64}e_{66}$	$(e_{11})e_{16}e_{61}e_{66}$

because the necessary fields in between the two branes are missing.

We have to emphasize again that the model presented in Sec. VI therefore represents the first compactification with intersecting D6-branes at angles and genuinely three generations, i.e., no brane recombination is required to obtain three quark and lepton families.

A similar reasoning applies to the left-right symmetric model displayed in Sec. VII .

It will be interesting to explore the whole class of discussed models with the given chiral spectrum in more detail, meaning that one could compare all different concrete realizations in a spirit like in [75]. Besides, the behavior of the Yukawa and gauge coupling constants

TABLE XXIV. Relation between orbits of fixed points and cycles as read off from (13).

2 − cycle ⊗ 1 − cycle	Exceptional 3-cycle
$e_{11} \otimes (n_3\pi_5 + m_3\pi_6)$	—
$e_{14} \otimes (n_3\pi_5 + m_3\pi_6)$	$n_3\varepsilon_2 + m_3\tilde{\varepsilon}_2$
$e_{15} \otimes (n_3\pi_5 + m_3\pi_6)$	$n_3(\tilde{\varepsilon}_2 - \varepsilon_2) - m_3\varepsilon_2$
$e_{16} \otimes (n_3\pi_5 + m_3\pi_6)$	$-n_3\tilde{\varepsilon}_2 - m_3(\tilde{\varepsilon}_2 - \varepsilon_2)$
$e_{41} \otimes (n_3\pi_5 + m_3\pi_6)$	$n_3\varepsilon_1 + m_3\tilde{\varepsilon}_1$
$e_{51} \otimes (n_3\pi_5 + m_3\pi_6)$	$n_3(\tilde{\varepsilon}_1 - \varepsilon_1) - m_3\varepsilon_1$
$e_{61} \otimes (n_3\pi_5 + m_3\pi_6)$	$-n_3\tilde{\varepsilon}_1 - m_3(\tilde{\varepsilon}_1 - \varepsilon_1)$
$e_{44} \otimes (n_3\pi_5 + m_3\pi_6)$	$n_3\varepsilon_3 + m_3\tilde{\varepsilon}_3$
$e_{45} \otimes (n_3\pi_5 + m_3\pi_6)$	$n_3\varepsilon_4 + m_3\tilde{\varepsilon}_4$
$e_{46} \otimes (n_3\pi_5 + m_3\pi_6)$	$n_3\varepsilon_5 + m_3\tilde{\varepsilon}_5$
$e_{54} \otimes (n_3\pi_5 + m_3\pi_6)$	$n_3(\tilde{\varepsilon}_5 - \varepsilon_5) - m_3\varepsilon_5$
$e_{55} \otimes (n_3\pi_5 + m_3\pi_6)$	$n_3(\tilde{\varepsilon}_3 - \varepsilon_3) - m_3\varepsilon_3$
$e_{56} \otimes (n_3\pi_5 + m_3\pi_6)$	$n_3(\tilde{\varepsilon}_4 - \varepsilon_4) - m_3\varepsilon_4$
$e_{64} \otimes (n_3\pi_5 + m_3\pi_6)$	$-n_3\tilde{\varepsilon}_4 - m_3(\tilde{\varepsilon}_4 - \varepsilon_4)$
$e_{65} \otimes (n_3\pi_5 + m_3\pi_6)$	$-n_3\tilde{\varepsilon}_5 - m_3(\tilde{\varepsilon}_5 - \varepsilon_5)$
$e_{66} \otimes (n_3\pi_5 + m_3\pi_6)$	$-n_3\tilde{\varepsilon}_3 - m_3(\tilde{\varepsilon}_3 - \varepsilon_3)$

depends on the internal geometry and the full massless spectrum. For instance, one could try to calculate the threshold corrections to these models as in [45] and determine if gauge coupling unification is possible [46]. Furthermore, supersymmetry breaking sources should arise at some point and might be understandable in these models. All these tasks hopefully will be achieved in the future [76].

ACKNOWLEDGMENTS

It is a pleasure to thank L. Görlich, K. Landsteiner, A. Uranga, K. Wendland, J. Cascales, W. Troost, A. van Proeyen, D. Lüst and especially R. Blumenhagen and L. Huiszoon for helpful discussions. This work is supported by the RTN programs under Contract Nos. HPRN-CT-2000-00131 and HPRN-CT-2000-00148 and in part also by the Federal Office for Scientific, Technical and Cultural Affairs through the "Interuniversity Attraction Poles Programme–Belgian Science Policy" P5/27.

APPENDIX A: BASIS FOR A $\mathbb{Z}_3$ INVARIANT 2-TORUS

We fix the angle between the two basis vectors of a $\mathbb{Z}_3$ invariant 2-torus to be $\pi/3$. With this restriction, the two possible $\mathcal{R}$ invariant lattices are spanned by

$$\begin{aligned} e_1^{\mathbf{A}} &= \begin{pmatrix} \sqrt{2} \\ 0 \end{pmatrix}, \qquad e_2^{\mathbf{A}} = \begin{pmatrix} 1/\sqrt{2} \\ \sqrt{3/2} \end{pmatrix}, \\ e_1^{*\mathbf{A}} &= \begin{pmatrix} 1/\sqrt{2} \\ -1/\sqrt{6} \end{pmatrix}, \qquad e_2^{*\mathbf{A}} = \begin{pmatrix} 0 \\ \sqrt{2/3} \end{pmatrix}, \end{aligned} \tag{A1}$$

for the **A** orientation where π_{2k-1} lies on the $\mathcal{R}$ invariant plane, and

$$\begin{aligned} e_1^{\mathbf{B}} &= \begin{pmatrix} \sqrt{3/2} \\ -1/\sqrt{2} \end{pmatrix}, \qquad e_2^{\mathbf{B}} = \begin{pmatrix} \sqrt{3/2} \\ 1/\sqrt{2} \end{pmatrix}, \\ e_1^{*\mathbf{B}} &= \begin{pmatrix} 1/\sqrt{6} \\ -1/\sqrt{2} \end{pmatrix}, \qquad e_2^{*\mathbf{B}} = \begin{pmatrix} 1/\sqrt{6} \\ 1/\sqrt{2} \end{pmatrix}, \end{aligned} \tag{A2}$$

for the **B** orientation where $\mathcal{R}$ exchanges π_{2k-1} and π_{2k}.

APPENDIX B: EXCEPTIONAL CYCLES, WRAPPING NUMBERS AND FIXED POINTS ON $T_1^2 \times T_2^2$

In this section, some technical details regarding the fractional branes are given. Table XXIV lists the corresponding fixed points which are possible to be traversed for a given set of geometric brane wrapping numbers and displacements. The connection between the orbits of the traversed fixed points and the corresponding exceptional cycles is subsequently given in Table XXIV.

APPENDIX C: SOME LOOP AN TREE-CHANNEL RESULTS

1. Tree-channel bulk part

The oscillator expansion of an untwisted boundary state (30) with spin structure $\eta = \pm 1$ and relative angles $\pi\varphi_a^k$ w.r.t. π_{2k-1} is given by [5,11]

$$\begin{aligned} |D6; (n_i^a, m_i^a), \eta\rangle \sim \exp\Big\{ &- \sum_{k=0}^{3}\sum_n \frac{e^{2\pi i \varphi_a^k}}{n} \alpha_{-n}^k \tilde{\alpha}_{-n}^k \\ &- i\eta \sum_{k=0}^{3}\sum_r e^{2\pi i \varphi_a^k} \psi_{-r}^k \tilde{\psi}_{-r}^k + h.c. \Big\} \\ &\times |0, \eta; p^k, w^k; \tau_i, \sigma_i\rangle. \end{aligned} \tag{C1}$$

In order to shorten the notation, the noncompact coordinates are denoted by $k = 0$ and the corresponding angle is $\varphi_a^0 \equiv 0$.

In addition to the Kaluza Klein momenta and windings existing in toroidal compactifications, for fractional branes discrete Wilson lines on $T_1^2 \times T_2^2$ parametrized by τ_1, τ_2 arise from the $\mathbb{Z}_2$ fixed points [36], see Eq. (28). A bulk brane can be displaced from the origin by $\sum_{i=1}^{6} \sigma_i \pi_i$, with arbitrary values $\sigma_i \in [0, 1)$, whereas for a fractional brane the displacement is discretized on two tori, $\sigma_i \in \{0, 1/2\}$ for $i = 1, \ldots, 4$.

Relative Wilson lines between two different boundary states which are parallel on a 2-torus give rise to complex phases at each mass level, i.e., if L is the dimensionless length of the 1-cycle wrapped by the two branes, R^2 the volume of the corresponding 2-torus, $\frac{\tau}{2} \in \{0, 1/2\}$ the relative Wilson line and σ the spatial separation, the tree-channel zero mode contributions are given by

$$\tilde{\mathcal{L}}(l) = \left(\sum_{r\in\mathbb{Z}} e^{-\pi l r^2 L^2 R^2/\alpha' + \pi i r\tau}\right)\left(\sum_{s\in\mathbb{Z}} e^{-\pi l s^2 L^2 \alpha'/R^4 + 2\pi i s\sigma}\right). \tag{C2}$$

Modular transformation leads to the loop channel annulus contribution

$$\mathcal{L}(t) = \left(\sum_{r\in\mathbb{Z}} e^{-2\pi t(r-\tau/2)^2\alpha'/(R^2L^2)}\right)\left(\sum_{s\in\mathbb{Z}} e^{-2\pi t(s-\sigma)^2 R^4/(L^2\alpha')}\right), \tag{C3}$$

which confirms that strings stretching between parallel branes with relative Wilson lines and/or spatial separation do not carry massless modes.

2. Tree-channel twisted part

The oscillator modding of a twisted boundary state (31) is shifted by the twist vector $v = (1/2, -1/2, 0)$,

$$\begin{aligned}|D6; (n_3^a, m_3^a), e_{ij}\eta\rangle \sim \exp\Bigg\{ &-\sum_{k=0,3}\sum_n \frac{e^{2\pi i\varphi_a^k}}{n}\alpha^k_{-n}\tilde{\alpha}^k_{-n} - i\eta\sum_{k=0,3}\sum_r e^{2\pi i\varphi_a^k}\psi^k_{-r}\tilde{\psi}^k_{-r} - \sum_{j=1,2}\sum_n \frac{e^{2\pi i\varphi_a^j}}{n}\alpha^j_{-n+v_j}\tilde{\alpha}^j_{-n+v_j} \\ &- i\eta\sum_{j=1,2}\sum_r e^{2\pi i\varphi_a^j}\psi^j_{-r+v_j}\tilde{\psi}^j_{-r+v_j} + h.c.\Bigg\}|0, \eta; p^3, w^3, e_{ij}\rangle,\end{aligned} \tag{C4}$$

and the discrete Wilson lines enter the boundary states only as relative signs α_{ij} between the twisted sector contributions, compare Eq. (31).

The cross-cap states do not have any twisted contributions.

3. Oscillator contributions to the amplitudes

The tree-channel oscillator contributions to the annulus and Möbius strip amplitude are of the form

$$\tilde{\mathcal{A}}^{\alpha\beta}_{v,(\varphi_1,\varphi_2,\varphi_3)} = \frac{\vartheta\begin{bmatrix}\alpha\\ \beta\end{bmatrix}}{\eta^3}\prod_{i=1}^3 \frac{\vartheta\begin{bmatrix}\alpha - v_i\\ \varphi_i+\beta\end{bmatrix}}{\vartheta\begin{bmatrix}1/2 - v_i\\ \varphi_i + 1/2\end{bmatrix}}(2l) \qquad \tilde{\mathcal{M}}^{\alpha\beta}_{(\varphi_1,\varphi_2,\varphi_3)} = \frac{\vartheta\begin{bmatrix}\alpha\\ \beta\end{bmatrix}}{\eta^3}\prod_{i=1}^3 \frac{\vartheta\begin{bmatrix}\alpha\\ \varphi_i+\beta\end{bmatrix}}{\vartheta\begin{bmatrix}1/2\\ \varphi_i + 1/2\end{bmatrix}}(2l - i/2) \tag{C5}$$

where $v = 0$ for the untwisted and $v = (1/2, -1/2, 0)$ for the $\mathbb{Z}_2$ twisted annulus contributions. $\alpha = 0, 1/2$ corresponds to $NS - NS$ and $R - R$ contributions, respectively, and $\beta = 0, 1/2$ labels contributions from identical and opposite spin structures. For more details on the notation see, e.g., the appendices of [4,10].

For each vanishing angle $\varphi_i = 0$ and vanishing twist v_i, the corresponding denominator has to be replaced,

$$\vartheta\begin{bmatrix}1/2\\ \varphi_i + 1/2\end{bmatrix} \xrightarrow{\varphi_i} \eta^3.$$

The loop channel oscillator contributions are given by

$$\mathcal{A}^{A,B}_{v,(\varphi_1,\varphi_2,\varphi_3)} = i\frac{\vartheta\begin{bmatrix}A\\ B\end{bmatrix}}{\eta^3}\prod_{i=1}^3 \frac{\vartheta\begin{bmatrix}A - \varphi_i\\ B - v_i\end{bmatrix}}{\vartheta\begin{bmatrix}1/2 - \varphi_i\\ 1/2 - v_i\end{bmatrix}}(t) \qquad \mathcal{M}^{A,B}_{(\varphi_1,\varphi_2,\varphi_3)} = i\frac{\vartheta\begin{bmatrix}A\\ B\end{bmatrix}}{\eta^3}\prod_{i=1}^3 \frac{\vartheta\begin{bmatrix}A + 2\varphi_i\\ B - \varphi_i\end{bmatrix}}{\vartheta\begin{bmatrix}1/2 + 2\varphi_i\\ 1/2 - \varphi_i\end{bmatrix}}(t - i/2) \tag{C6}$$

where $v = 0$ corresponds to an open string state without and $v = (1/2, -1/2, 0)$ with $\mathbb{Z}_2$ insertion. The modification for vanishing angle is identical to the tree-channel result up to a factor of i.

The modular transformation $l = 1/(\kappa t)$ (where $\kappa = 2$ or 8 for the annulus or Möbius strip, respectively) for three nonvanishing angles is given by

$$\tilde{\mathcal{A}}^{\alpha\beta}_{v,(\varphi_1,\varphi_2,\varphi_3)} = \frac{e^{\pi i(2\alpha-1)\sum_{i=1}^3\varphi_i}}{t}\mathcal{A}^{\beta,\alpha}_{v,(\varphi_1,\varphi_2,\varphi_3)}, \qquad \tilde{\mathcal{M}}^{\alpha\beta}_{(\varphi_1,\varphi_2,\varphi_3)} = \frac{e^{2\pi i\alpha}}{2}\frac{e^{4(\alpha+\beta)\pi i\sum_{i=1}^3\varphi_i}}{t}\mathcal{M}^{\alpha,1/2-(\alpha+\beta)}_{(\varphi_1,\varphi_2,\varphi_3)}. \tag{C7}$$

Each vanishing angle modifies these equations by a factor of $1/t$ for the annulus and $1/(2t)$ for the Möbius strip.

APPENDIX D: SOME RESULTS FOR $T^6/(\mathbb{Z}_6 \times \mathbb{Z}_3)$

The orbifold generators Θ and ω are represented by the two shift vectors $v = (1/6, -1/6, 0)$ and $w = (0, 1/3, -1/3)$, respectively. The Hodge numbers are given by (see, e.g., [77] and also [10] for the closed string spectrum)

$$\begin{aligned} h^U_{1,1} &= 3, \quad h^{\Theta^3}_{1,1} = 4, \quad h^{\text{fixplanes}-\text{not}-\mathbb{Z}_2}_{,11} = 36, \quad h^{\text{fixpoints}}_{1,1} = 30 \\ h^U_{2,1} &= 0, \quad h^{\Theta^3}_{2,1} = 1, \quad h^{\text{fixplanes}-\text{not}-\mathbb{Z}_2}_{2,1} = 0, \quad h^{\text{fixpoints}}_{2,1} = 0. \end{aligned} \tag{D1}$$

The allowed compactification lattices are as depicted in Fig. 1, and the fundamental bulk 3-cycles can be chosen to be identical (up to normalization) to those displayed in Eq. (4). The orbits of wrapping numbers which describe all possible factorizable 3-cycles are given by

$$\begin{aligned} &\begin{pmatrix} n_1 & m_1 \\ n_2 & m_2 \\ n_3 & m_3 \end{pmatrix} \xrightarrow{\Theta} \begin{pmatrix} -m_1 & n_1 + m_1 \\ (n_2 + m_2) & -n_2 \\ n_3 & m_3 \end{pmatrix} \xrightarrow{\Theta} \begin{pmatrix} -(n_1 + m_1) & n_1 \\ m_2 & -(n_2 + m_2) \\ n_3 & m_3 \end{pmatrix} \\ &\downarrow \omega \\ &\begin{pmatrix} n_1 & m_1 \\ -(n_2 + m_2) & n_2 \\ m_3 & -(n_3 + m_3) \end{pmatrix} \xrightarrow{\Theta} \begin{pmatrix} -m_1 & n_1 + m_1 \\ -m_2 & (n_2 + m_2) \\ m_3 & -(n_3 + m_3) \end{pmatrix} \xrightarrow{\Theta} \begin{pmatrix} -(n_1 + m_1) & n_1 \\ n_2 & m_2 \\ m_3 & -(n_3 + m_3) \end{pmatrix} \\ &\downarrow \omega \\ &\begin{pmatrix} n_1 & m_1 \\ m_2 & -(n_2 + m_2) \\ -(n_3 + m_3) & n_3 \end{pmatrix} \xrightarrow{\Theta} \begin{pmatrix} -m_1 & n_1 + m_1 \\ -n_2 & -m_2 \\ -(n_3 + m_3) & n_3 \end{pmatrix} \xrightarrow{\Theta} \begin{pmatrix} -(n_1 + m_1) & n_1 \\ -(n_2 + m_2) & n_2 \\ -(n_3 + m_3) & n_3 \end{pmatrix} \end{aligned} \tag{D2}$$

and lead (up to normalization) to the coefficients (6) computed for the $T^6/\mathbb{Z}_6$ case. Only two exceptional 3-cycles arise. The fixed points on T^2_1 are permuted under Θ as in (10) and are fixed under ω. On T^2_2, the permutations are given by

$$\Theta(4) = \omega(4) = 6, \qquad \Theta(5) = \omega(5) = 4, \qquad \Theta(6) = \omega(6) = 5. \tag{D3}$$

On T^2_3, only ω fixed points occur, which transform trivially under Θ and do not contribute to exceptional 3-cycles. Two linearly independent, orbifold invariant exceptional 3-cycles with vanishing self-intersection can be expressed in terms of (13),

$$\begin{aligned} \zeta_1 &= (1 + \Theta + \Theta^2)(1 + \omega + \omega^2)e_{44} \otimes \pi_5 \sim \varepsilon_3 - \varepsilon_4 + \tilde{\varepsilon}_4 - \tilde{\varepsilon}_5, \\ \zeta_2 &= (1 + \Theta + \Theta^2)(1 + \omega + \omega^2)e_{55} \otimes \pi_5 \sim -\varepsilon_3 + \varepsilon_5 + \tilde{\varepsilon}_3 - \tilde{\varepsilon}_4. \end{aligned} \tag{D4}$$

[1] M. Berkooz, M. R. Douglas, and R. G. Leigh, Nucl. Phys. **B480**, 265 (1996).
[2] Augusto Sagnotti, hep-th/0208020.
[3] Ralph Blumenhagen, Lars Görlich, and Boris Körs, hep-th/0002146.
[4] Ralph Blumenhagen, Lars Görlich, and Boris Körs, J. High Energy Phys. 01 (2000) 040.
[5] Ralph Blumenhagen, Lars Görlich, Boris Körs, and Dieter Lüst, J. High Energy Phys. 10 (2000) 006.
[6] Ralph Blumenhagen, Boris Körs, and Dieter Lüst, J. High Energy Phys. 02 (2001) 030.
[7] C. Angelantonj, Ignatios Antoniadis, E. Dudas, and A. Sagnotti, Phys. Lett. B **489**, 223 (2000).
[8] G. Aldazabal, S. Franco, Luis E. Ibanez, R. Rabadan, and A. M. Uranga, J. High Energy Phys. 02 (2001) 047.
[9] G. Aldazabal, S. Franco, Luis E. Ibanez, R. Rabadan, and A. M. Uranga, J. Math. Phys. (N.Y.) **42**, 3103 (2001).
[10] Stefan Förste, Gabriele Honecker, and Ralph Schreyer, Nucl. Phys. **B593**, 127 (2001) .
[11] Stefan Förste, Gabriele Honecker, and Ralph Schreyer, J. High Energy Phys. 06 (2001) 004.
[12] Shamit Kachru and John McGreevy, Phys. Rev. D **61**, 026001 (2000).
[13] Angel M. Uranga, Classical Quantum Gravity **20**, S373 (2003).
[14] Tassilo Ott, Fortschr. Phys. **52**, 28 (2004).

[15] Fernando G. Marchesano Buznego, Ph.D. thesis, Departamento de Fisica Teorica, Universidad Autonoma de Madrid (hep-th/0307252).
[16] Lars Görlich, Ph.D. thesis, Humboldt University at Berlin (hep-th/0401040).
[17] Carlo Angelantonj and Augusto Sagnotti, Phys. Rep. **371**, 1 (2002); **376**, 339(E) (2003).
[18] Ralph Blumenhagen, Volker Braun, Boris Körs, and Dieter Lüst, J. High Energy Phys. 07 (2002) 026.
[19] Ralph Blumenhagen, Volker Braun, Boris Körs, and Dieter Lüst, hep-th/0210083.
[20] Luis E. Ibanez, F. Marchesano, and R. Rabadan, J. High Energy Phys. 11 (2001) 002.
[21] Christos Kokorelis, J. High Energy Phys. 08 (2002) 018.
[22] Christos Kokorelis, J. High Energy Phys. 09 (2002) 029.
[23] Ralph Blumenhagen, Boris Körs, Dieter Lüst, and Tassilo Ott, Nucl. Phys. **B616**, 3 (2001).
[24] Ralph Blumenhagen, Boris Körs, Dieter Lüst, and Tassilo Ott, Fortschr. Phys. **50**, 843 (2002).
[25] R. Rabadan, Nucl. Phys. **B620**, 152 (2002).
[26] Ralph Blumenhagen, Boris Körs, Dieter Lüst, and Tassilo Ott, Nucl. Phys. **B641**, 235 (2002).
[27] Juan Garcia-Bellido, Raul Rabadan, and Frederic Zamora, J. High Energy Phys. 01 (2002) 036.
[28] Mirjam Cvetic, Gary Shiu, and Angel M. Uranga, Phys. Rev. Lett. **87**, 201801 (2001).
[29] Mirjam Cvetic, Gary Shiu, and Angel M. Uranga, Nucl. Phys. **B615**, 3 (2001).
[30] Mirjam Cvetic, Ioannis Papadimitriou, and Gary Shiu, Nucl. Phys. **B659**, 193 (2003).
[31] Mirjam Cvetic and Ioannis Papadimitriou, Phys. Rev. D **67**, 126006 (2003).
[32] Mirjam Cvetic, Tianjun Li, and Tao Liu, hep-th/0403061.
[33] Marianna Larosa and Gianfranco Pradisi, Nucl. Phys. **B667**, 261 (2003).
[34] Mirjam Cvetic, Paul Langacker, and Gary Shiu, Phys. Rev. D **66**, 066004 (2002).
[35] Mirjam Cvetic, Paul Langacker, and Gary Shiu, Nucl. Phys. **B642**, 139 (2002).
[36] Ralph Blumenhagen, Lars Görlich, and Tassilo Ott, J. High Energy Phys. 01 (2003) 021.
[37] Gabriele Honecker, Nucl. Phys. **B666**, 175 (2003).
[38] Gabriele Honecker, hep-th/0309158.
[39] D. Cremades, L. E. Ibanez, and F. Marchesano, J. High Energy Phys. 07 (2002) 009.
[40] D. Cremades, L. E. Ibanez, and F. Marchesano, hep-ph/0212048.
[41] Christos Kokorelis, hep-th/0212281.
[42] Christos Kokorelis, hep-th/0309070.
[43] Edward Witten, hep-th0212247.
[44] Igor R. Klebanov and Edward Witten, Nucl. Phys. **B664**, 3 (2003).
[45] D. Lüst and S. Stieberger, hep-th/0302221.
[46] Ralph Blumenhagen, Dieter Lüst, and Stephan Stieberger, J. High Energy Phys. 07 (2003) 036.
[47] D. Cremades, L. E. Ibanez, and F. Marchesano, hep-ph/0212064.
[48] Boris Körs and Pran Nath, Phys. Lett. B **586**, 366 (2004).
[49] Noriaki Kitazawa, hep-th/0403278.
[50] D. Cremades, L. E. Ibanez, and F. Marchesano, J. High Energy Phys. 07 (2002) 022.
[51] D. Cremades, L. E. Ibanez, and F. Marchesano, J. High Energy Phys. 07 (2003) 038.
[52] Mirjam Cvetic and Ioannis Papadimitriou, Phys. Rev. D **68**, 046001 (2003); **70** 029903(E) (2004).
[53] S. A. Abel and A.W. Owen, Nucl. Phys. **B663**, 197 (2003).
[54] Mirjam Cvetic, Paul Langacker, and Jing Wang, Phys. Rev. D **68**, 046002 (2003).
[55] Boris Körs and Pran Nath, Nucl. Phys. **B681**, 77 (2004).
[56] Jan Louis, Ilka Brunner, and Stephan J. Huber, hep-ph/9811341.
[57] Dieter Lüst, Classical Quantum Gravity **21**, S1399 (2004).
[58] D. Lüst, Prog. Theor. Phys. Suppl. **152**, 59 (2004).
[59] Ralph Blumenhagen, J. High Energy Phys. 11 (2003) 055.
[60] Ralph Blumenhagen and Timo Weigand, J. High Energy Phys. 02 (2004) 041.
[61] Ralph Blumenhagen and Timo Weigand, Phys. Lett. B **591**, 161 (2004).
[62] G. Aldazabal, E. C. Andres, M. Leston, and C. Nunez, J. High Energy Phys. 09 (2003) 067.
[63] G. Aldazabal, E. C. Andres, and J. E. Juknevich, J. High Energy Phys. 05 (2004) 054.
[64] T. P. T. Dijkstra, L. R. Huiszoon, and A. N. Schellekens, hep-th/0403196.
[65] L. R. Huiszoon, Ph.D. thesis, Nijmegen University, 2002.
[66] Lance J. Dixon, Jeffrey A. Harvey, C. Vafa, and Edward Witten, Nucl. Phys. **B261**, 678 (1985).
[67] Lance J. Dixon, Jeffrey A. Harvey, C. Vafa, and Edward Witten, Nucl. Phys. **B274**, 285 (1986).
[68] Duiliu-Emanuel Diaconescu, Michael R. Douglas, and Jaume Gomis, J. High Energy Phys. 02 (1998) 013.
[69] Duiliu-Emanuel Diaconescu and Jaume Gomis, J. High Energy Phys. 10 (2000) 001.
[70] Mirjam Cvetic, Angel M. Uranga, and Jing Wang, Nucl. Phys. **B595**, 63 (2001).
[71] Matteo Bertolini, Int. J. Mod. Phys. A **18**, 5647 (2003).
[72] G. Aldazabal, A. Font, Luis E. Ibanez, and G. Violero, Nucl. Phys. **B536**, 29 (1998).
[73] Matthias Klein and Raul Rabadan, Nucl. Phys. **B596**, 197 (2001).
[74] P. Griffiths and J. Harris *Principles of Algebraic Geometry* (Wiley, New York, 1978).
[75] Michael R. Douglas. J. High Energy Phys. 05 (2003) 046.
[76] Gabriele Honecker and Tassilo Ott (work in progress).
[77] Matthias Klein and Raul Rabadan, J. High Energy Phys. 10 (2000) 049.